Semiconductor nanowire arrays for next generation highly integrated photonic systems and IoTs

Lan Fu
(lan.fu@anu.edu.au)

ARC Centre of Excellent of Transformative Meta-optical Systems (TMOS)
Department of Electronic Materials Engineering
Research School of Physics
The Australian National University

III-V Materials & Devices - Low Dimensional Materials (QWs, QDs, NWs, 2D)

Lasers/LEDs (blue-infrared)

Photodetetors (UV-THz)

Solar cells

Water splitting - hydrogen

Chemical Sensors

III-V compound semiconductors

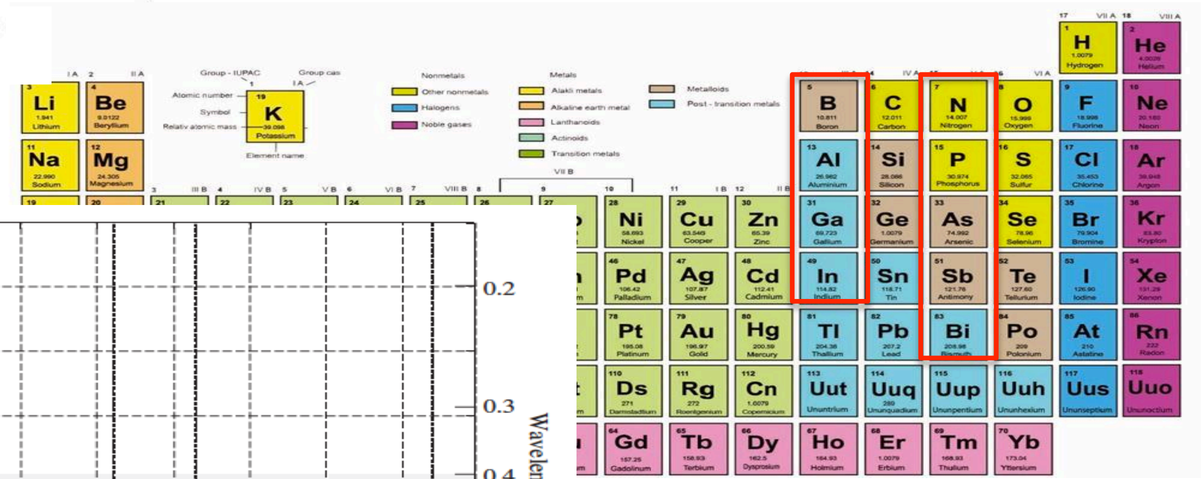

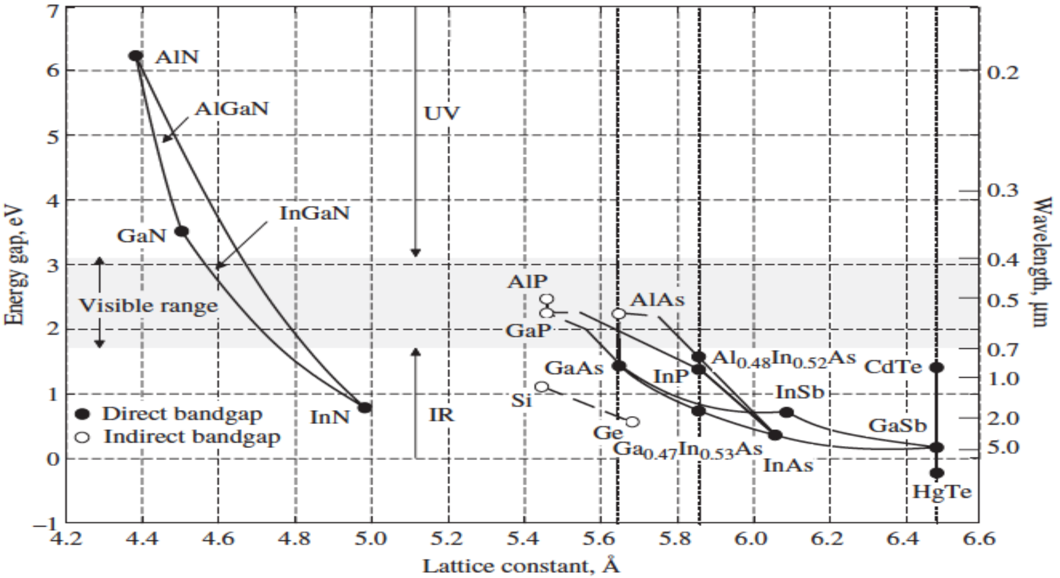

- Direct bandgap
- Excellent electron mobility
- Tunable alloy compositions/ bandgap (UV-MIR)

Australian National University

TMOS
ARC CENTRE OF EXCELLENCE FOR TRANSFORMATIVE META-OPTICAL SYSTEMS

Optoelectronic devices based on III-Vs

LEDs/Lasers

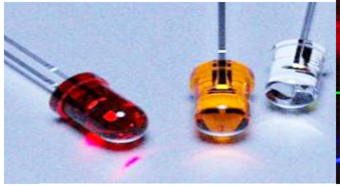

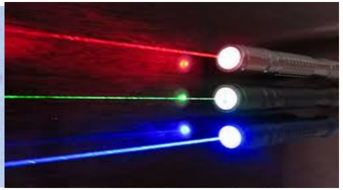

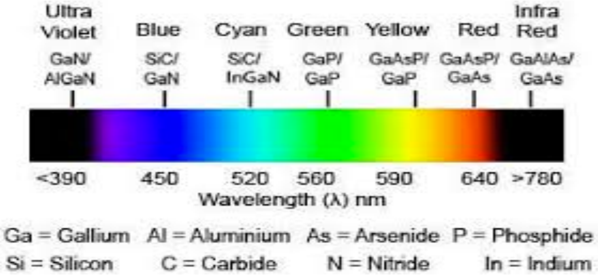

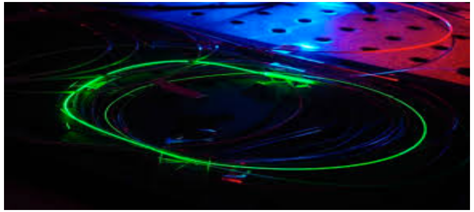

Photodetectors

InGaAs Photodiode

Thermal imaging camera (GaAs/AlGaAs QWIP)

Solar cells

Satellite Powered by Triple Junction Solar Cells

Concentrator PV

Highly functional and compact system: photonic/electronic integration

Optical interconnects

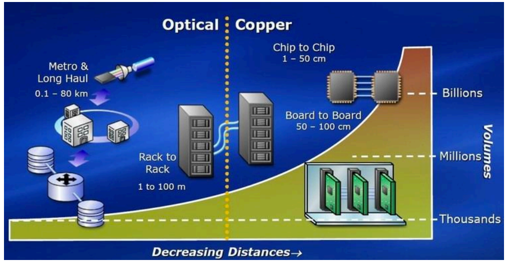

https://www.openpr.com

LiDAR (Light Detection and Ranging) technologies

Remote sensing

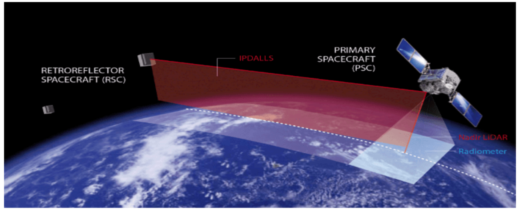

LIDAR Installed in Satellites for Remote Sensing

Autonomous vehicle

www.forbes.com

Smart Phone

iPhone12 Pro:
LiDAR Scanner

AR/VR/Hologram

https://theconversation.com/

Wireless sensor networks

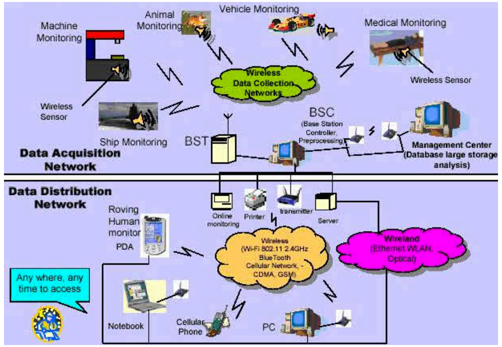

- Transport
- Industry
- …
- Agriculture
- Health

https://www.elprocus.com/

Material platforms for PICs/IoTs

Si based PICs

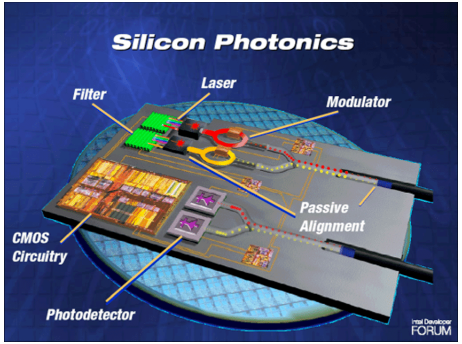

https://ic.tweakimg.net/ext/i.dsp/1109883395.png

InP based PICs

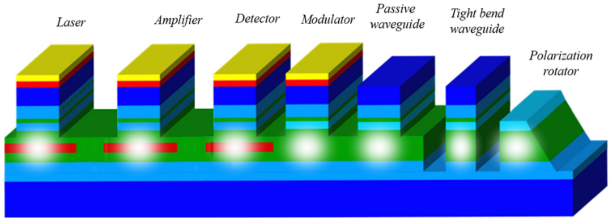

APL Photon. 4, 050901 (2019).

2D materials for PICs

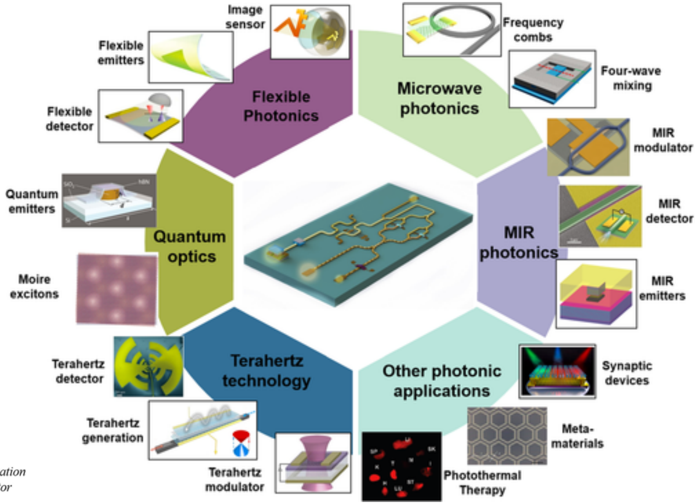

J. H. Wu, Small Science 1, 2000053 (2020).

Multiplexed wearable point-of-care testing

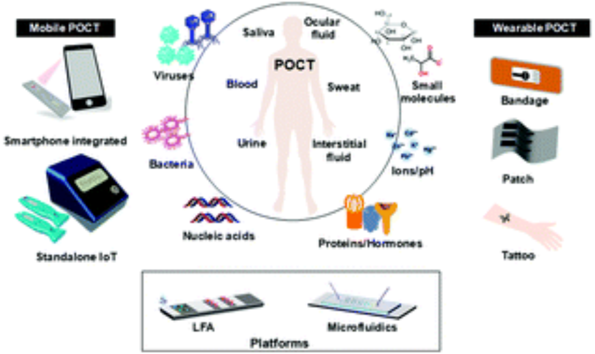

Chem. Soc. Rev., 2020,49, 1812.

III-V nanowires - a versatile, flexible material platform for PICs & IoTs

Outlines

- Introduction
- III-V NW materials and devices
- Quantum well nanowire array
  - SAE growth
  - Light emitting diodes
  - Photodetectors
- Nanowire array gas sensors (health and environmental monitoring)
  - NO_2
  - Acetone
- Conclusions

III-V nanowires as nano-building blocks for future PICs & IoTs

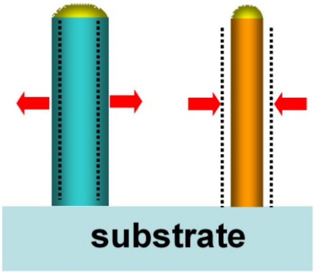

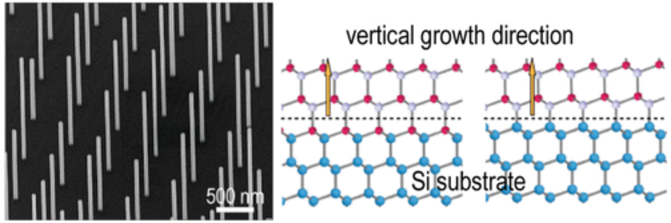

Nano Lett. 8, 3475 (2008).

- Relax the fundamental limitation of lattice mismatch
  - heterostructure growth/III-V on Si

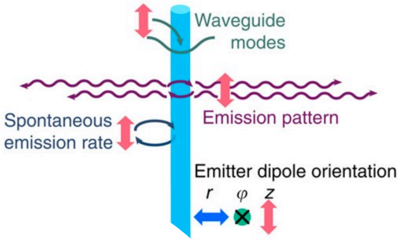

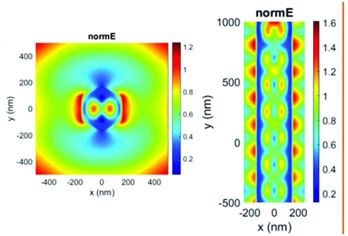

Nat Comm. 7, 13950 (2016). Nanoscale 14, 3527 (2022).

- Support both localized resonances and guided modes to enhance light emission and absorption

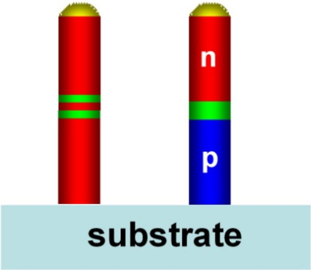

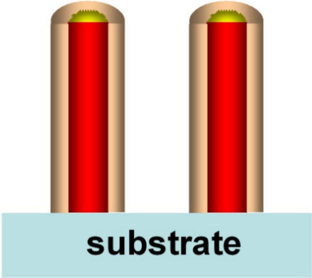

- Flexibility in device engineering in both axial and radial directions

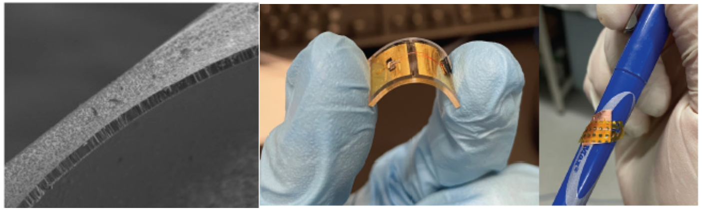

- Large surface area and mechanical flexibility for sensor or photo-electrochemical applications

III-V nanowire materials: growth/fabrication

- Bottom up: Epitaxial growth

Vapour-liquid-solid (VLS)

Selective area epitaxy (SAE)

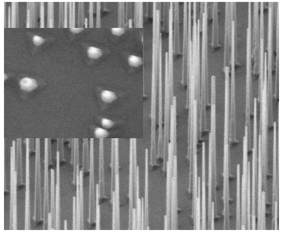

Nanoscale Res. Lett. 1, 208 (2016).

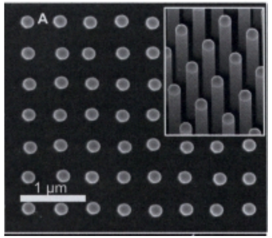

Science 339, 1057 (2013).

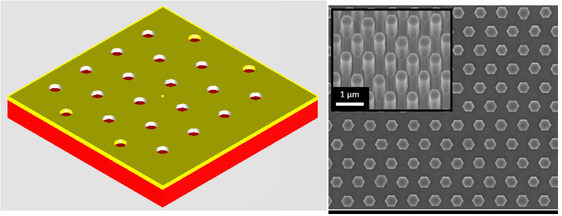

Y. Yang et al, ACS Nano 12, 10374, (2018).

- Top-down: etching

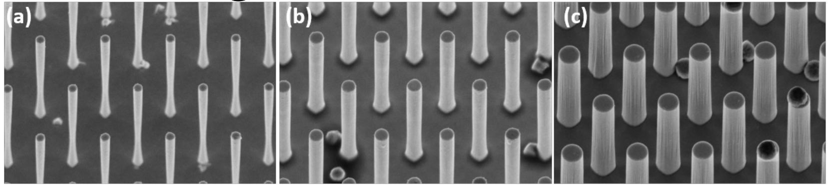

S. Y. Wei et al, Adv. Func. Mater. 32, 2107596 (2021).

Nanowire Devices: single vs array

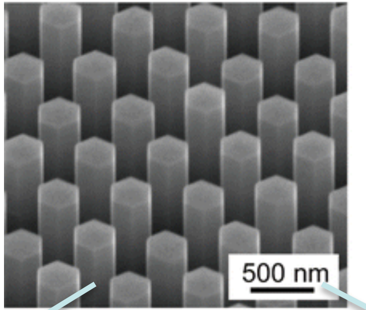

Single NW devices

Array NW devices

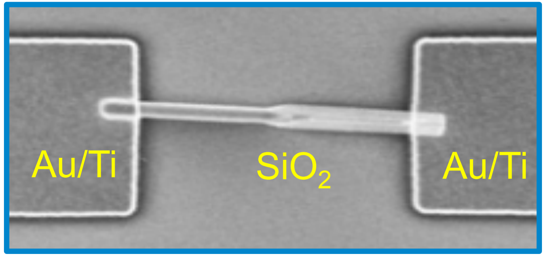

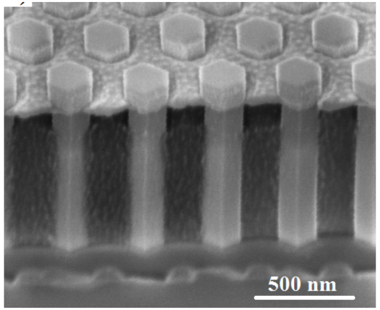

- Lasers/LEDs
- Detectors
- Solar cells
- Chemiresistive sensors

III-V Nanowire Materials and Devices

NW materials

SAE InP NWs

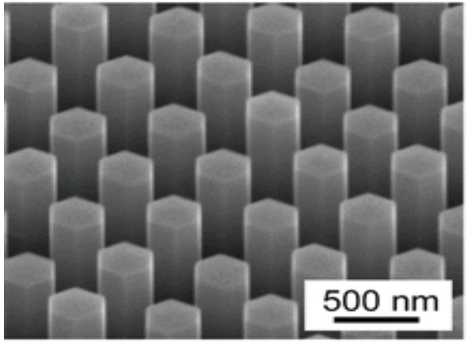

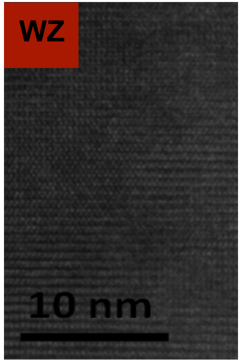

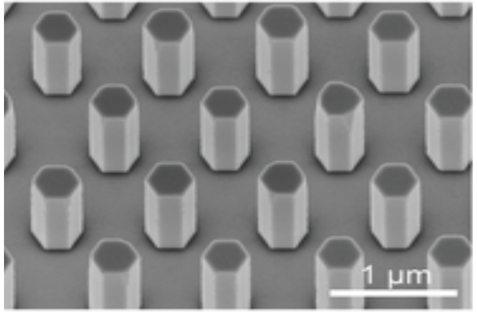

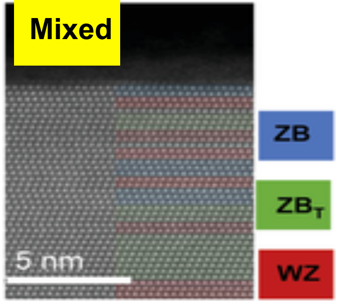

SAE InAs NWs

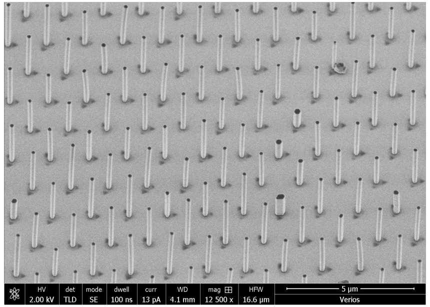

VLS GaAsSb NWs

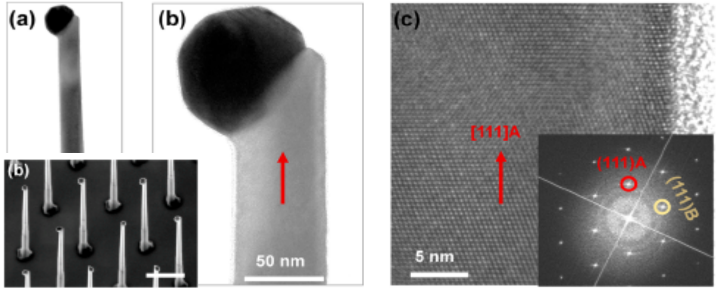

Top-down etched InP NWs

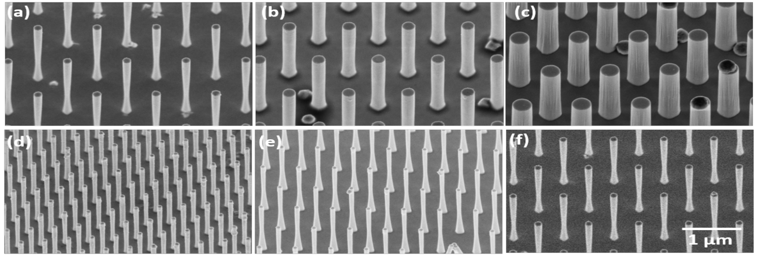

- A range of III-V NW materials including InP (WZ, WZ/ZB), GaAsSb, InAs, GaAs/AlGaAs QWs, and InGaAs/InP QWs etc

Single NW devices

Optically pumped laser

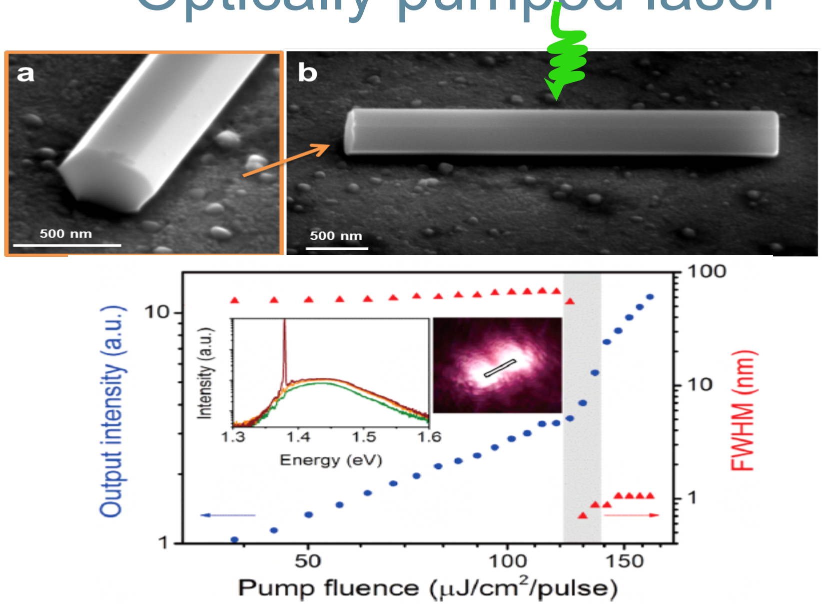

Q. Gao et al, Nano Lett. 14, 5206 (2014).

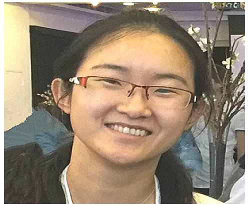

Integrating a nanowire laser in an on-chip photonic waveguide, R. Yi et al Nano Letters 22, 9920 (2022).
Vertical Emitting Nanowire Vector Beam Lasers, X. Zhang et al, ACS nano (2023).
Self-frequency-conversion nanowire lasers
R Yi et al, Light: Science & Applications 11, 120 (2022).
Ultralow threshold, single-mode InGaAs/GaAs multiquantum disk nanowire lasers
X Zhang et al, ACS nano 15, 9126 (2021).
Vertically emitting indium phosphide nanowire lasers, W. Z. Xu et al, Nano letters 18, 3414 (2018).

- 1D structure supports guided modes along the NW and providing optical feedback due to the large refractive index contrast at NW ends
- Room temperature lasing from the NWs transferred onto a low index substrate

Electrically injected laser remains challenging.

NW THz detector

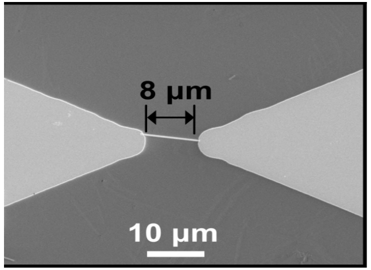

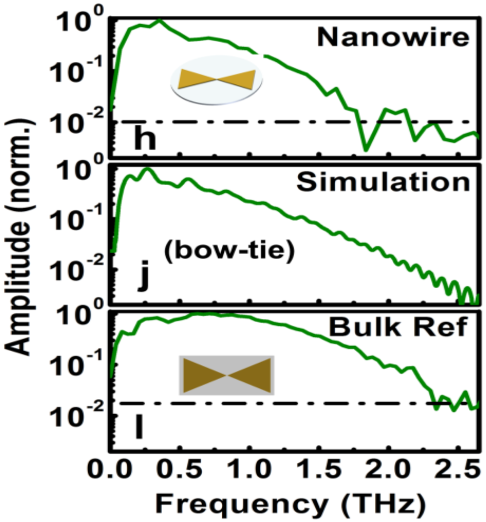

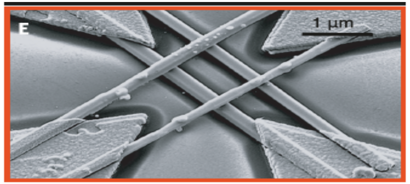

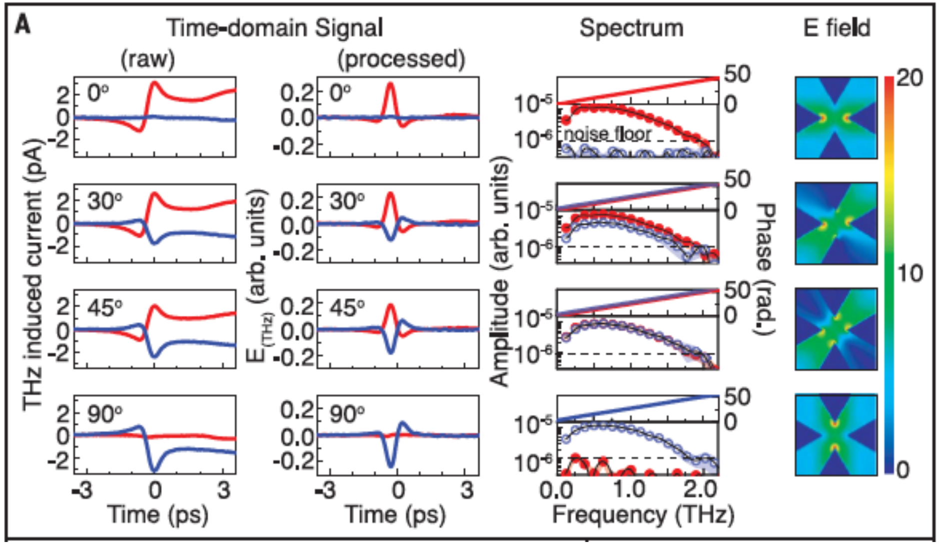

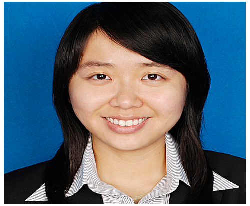

K. Peng et al., Nano Lett. 15, 206 (2015).
K. Peng et al., Nano Lett. 16, 4925 (2016).
K. Peng et al., Science 368, 510 (2020).

In collaboration with University of Oxford and University of Strathclyde

PN Junction design and characterisation for nanowire solar cells

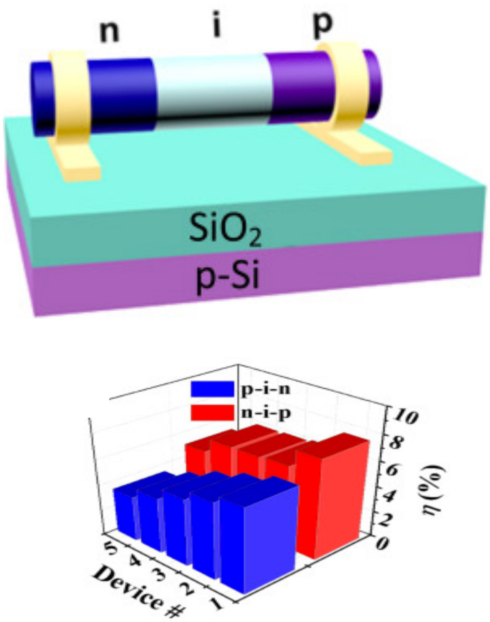

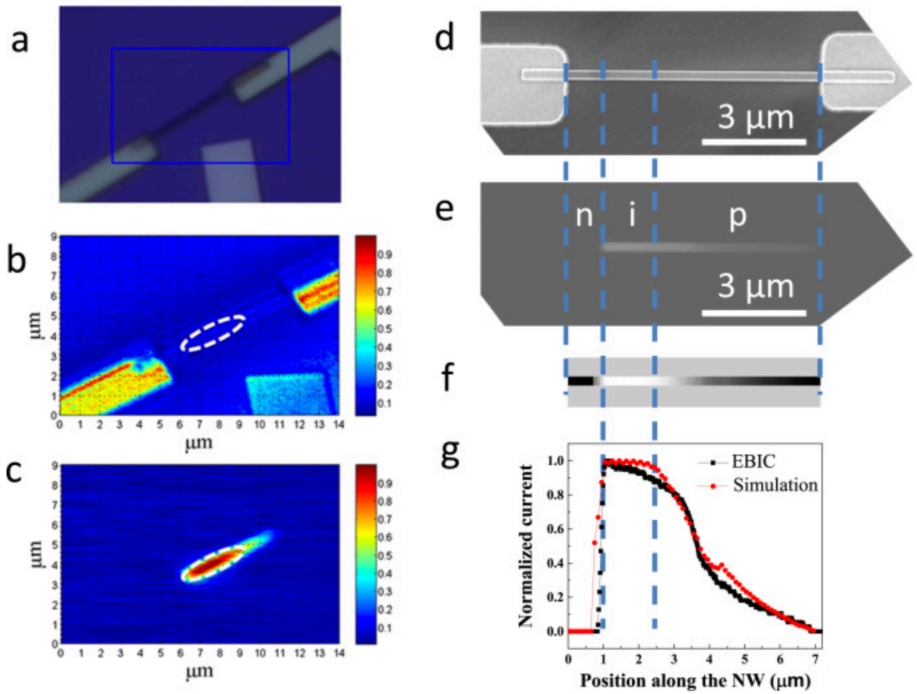

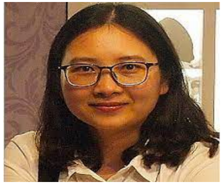

Z. Zhong, Z. Y. Li et al, Nano Energy 28, 106, (2016).
Z. Y. Li et al, Advanced Materials Technologies 3, 1800005 (2018).
Z Li, et al, Progress in Natural Science: Materials International 28, 178 (2018).

Nanowire Array Design

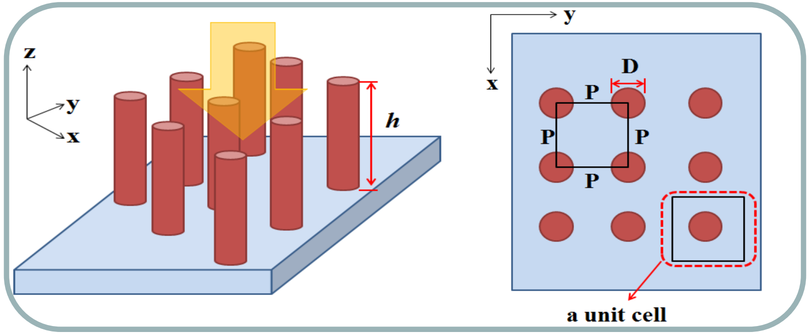

- Optical: the geometry (diameter, spacing, height and shape) of the NW array strongly affects its absorption and/or light emission characteristics.

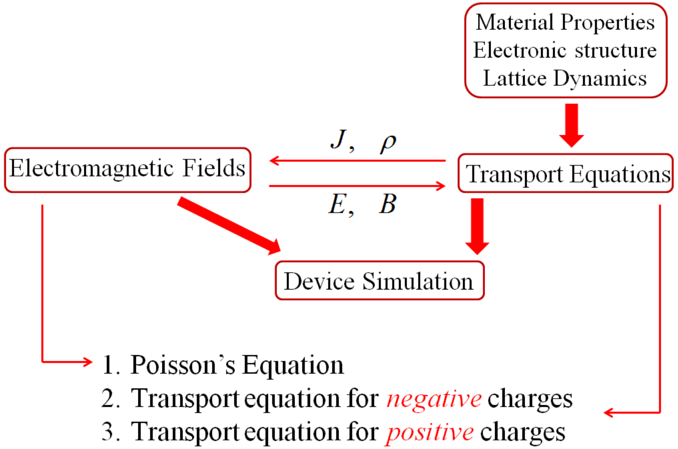

- Electrical: the design of the **electronic** (such as heterostructures/QWs) and **electrical** structures (such as pn junctions) of the NWs are also essential to achieve high performance NW devices.

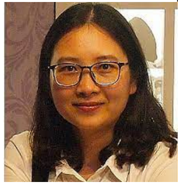

GaAsSb nanowire array dual-band multi-wavelength detectors

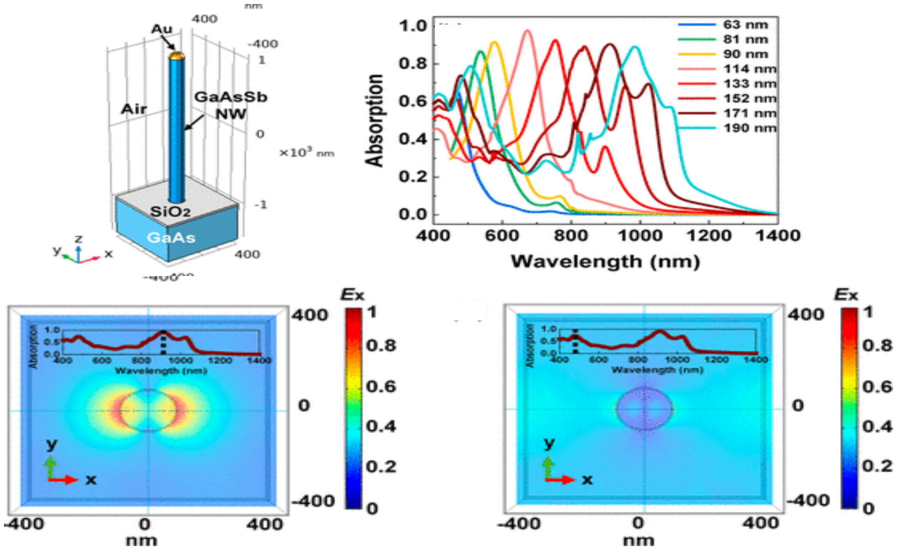

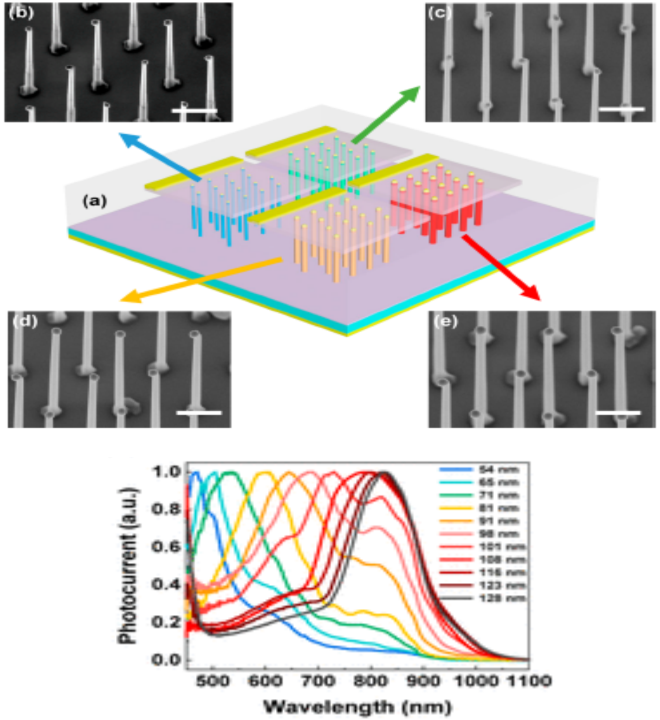

Z. Y. Li et al, Nano Letters , 21, 7388 (2021).

Australian National University

TMOS
ARC CENTRE OF EXCELLENCE FOR TRANSFORMATIVE META-OPTICAL SYSTEMS

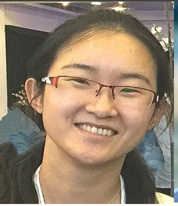

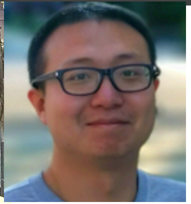

Nanowire array solar cells

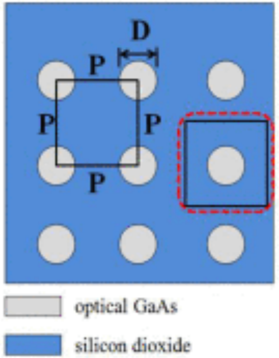

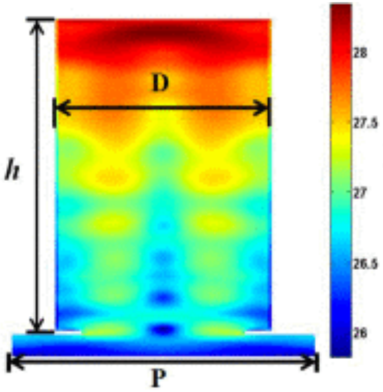

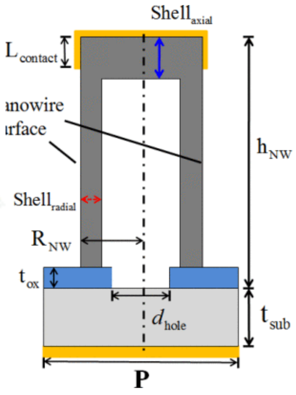

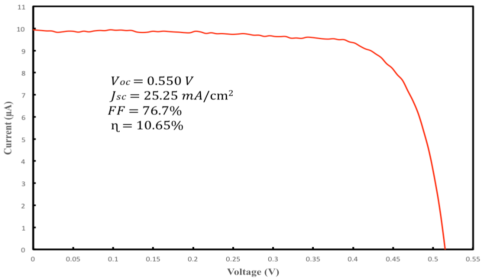

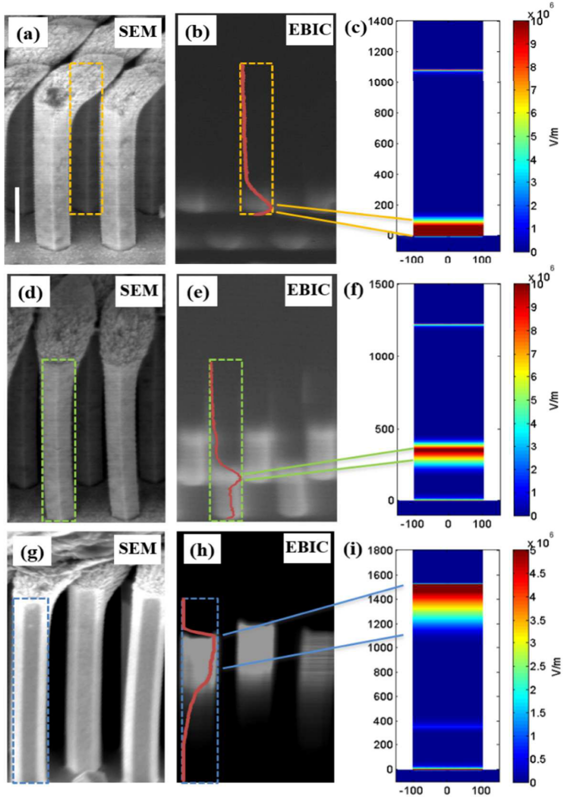

Z. Li et al, IEEE J. Photovoltaics 5, 854 (2015).
Q. Gao et al, Progress in Photovoltaics: Research & Applications 27, 237(2019).
Z. Y. Li et al, Advanced Materials Technologies 3, 1800005 (2018).

Top-down: p-InP/n-ZnO/AZO radial heterojunction NW solar cells

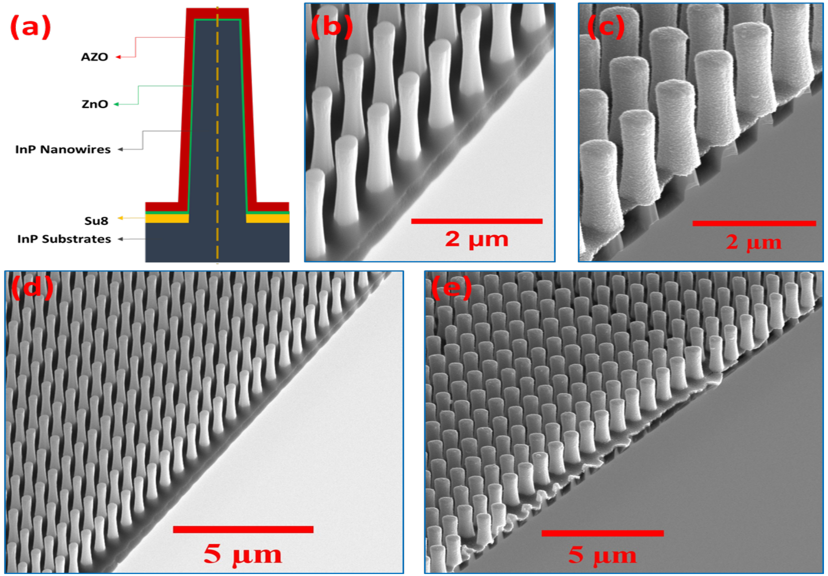

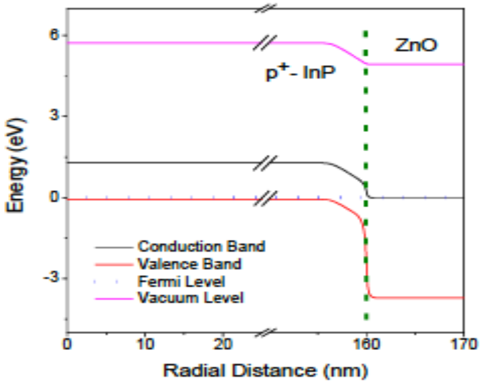

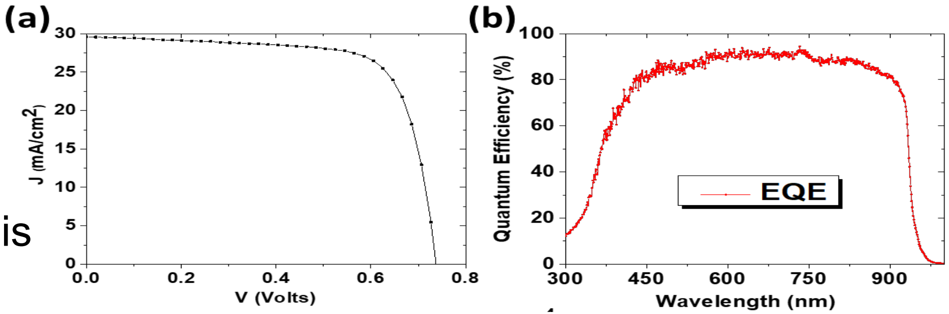

A photovoltaic conversion efficiency of 17.1% is achieve - the best reported value for radial junction nanowire solar cells.

V. Raj et al, ACS Nano 13, 12015 (2019).

Australian National University

TMOS
ARC CENTRE OF EXCELLENCE FOR TRANSFORMATIVE META-OPTICAL SYSTEMS

Radial heterojunction self-powered detector for single photon level photon detection

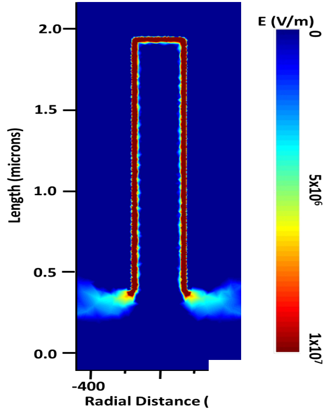

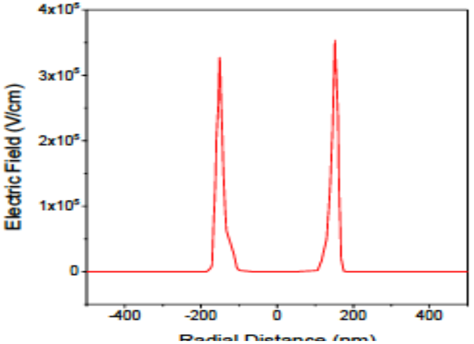

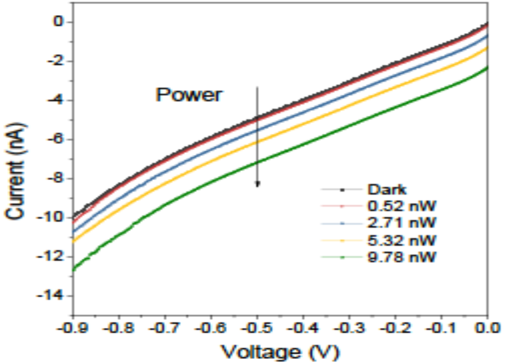

Self-powered detection (0 V) @700 nm picosecond laser (6 ps pulse width)

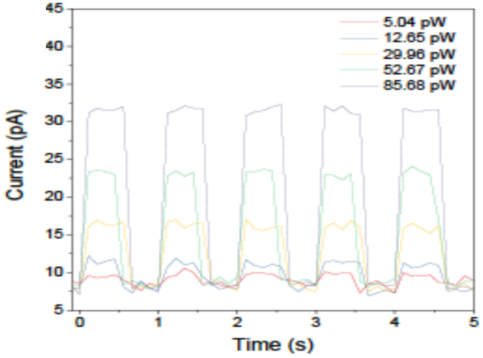

Y. Zhu, V. Raj et al, Advanced Materials 33, 2105729 (2021).

Quantum Well Nanowire Arrays

Quantum wells for optoelectronic device applications

- A semiconductor quantum well is a heterostructure formed by sandwiching a thin layer of small bandgap semiconductor with two layers of large bandgap semiconductor, such as GaAs/AlGaAs, or InGaAs/InP.
- Advantages of quantum wells
  - quantum confinement effect
  - band gap engineering

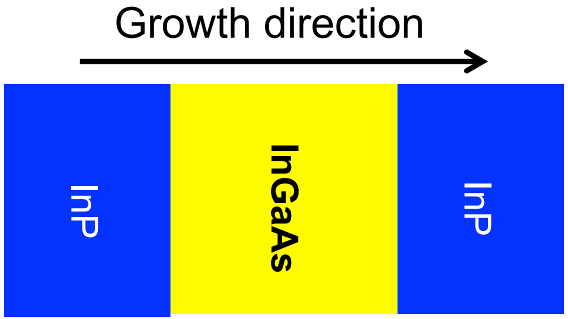

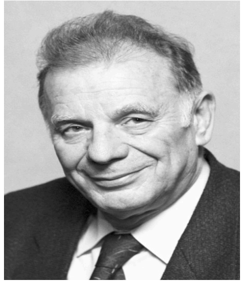

Zhores Alferov

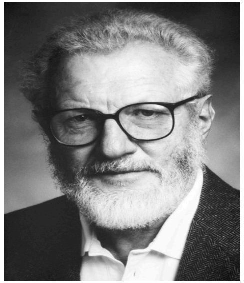

Herbert Kroemer

- Nobel Prizes 2000: “developing semiconductor heterostructures used in high-speed- and opto-electronics”.

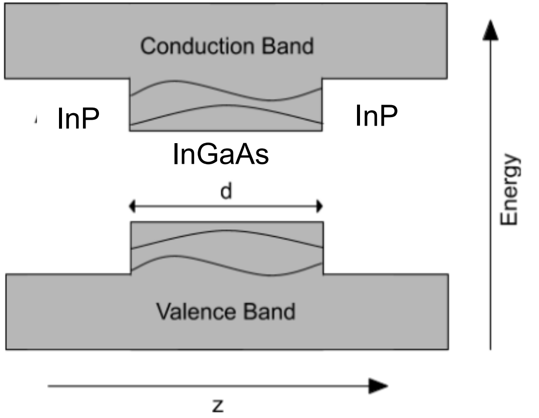

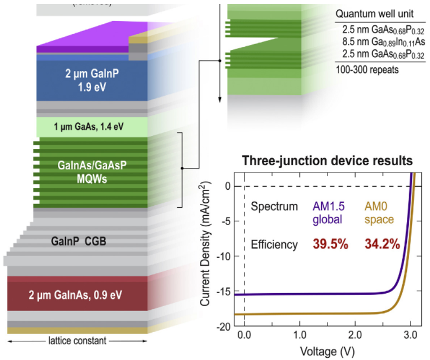

France et al., Joule 6, 1121–1135 (2022)

QW solar cell:

Triple junctions -
Record efficiency 39.5%

Mid- to long- wavelength QW infrared photodetector for thermal imaging

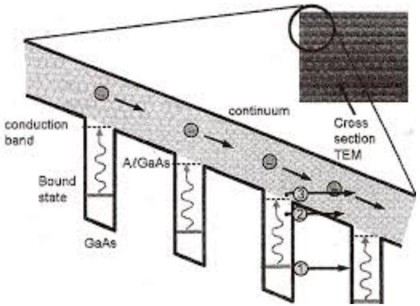

Sensors and Materials 12, 327 (2000).

NASA News: https://www.nasa.gov/centers/goddard/news/topstory/2006/qwip_advance.html

QW lasers:/LEDs

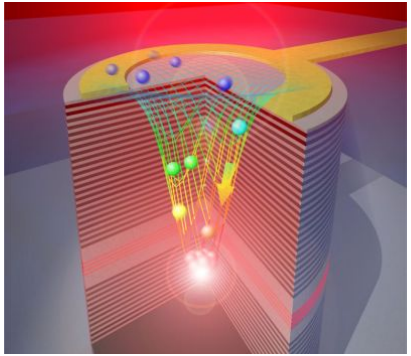

Schneider, C *et al.* . *Nature* **497,** 348 (2013).

- InGaAs/InP quantum wells have been widely used in laser diodes for telecommunication systems (1300-1600 nm).
- Incorporation of quantum wells in nanowires will further enhance the light emission and extraction efficiency, as well as wavelength tunability of LEDs.

QW-NW Array Growth

Australian National University

TMOS ARC CENTRE OF EXCELLENCE FOR TRANSFORMATIVE META-OPTICAL SYSTEMS

Nanowire array – selective area epitaxy (SAE)

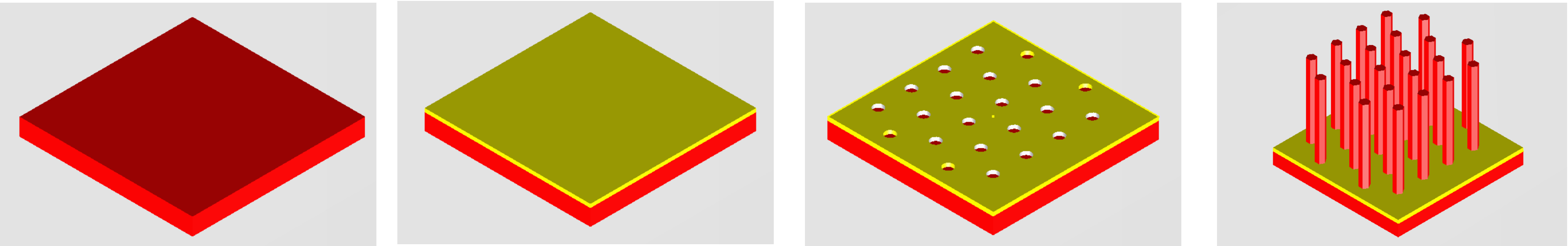

InP substrate | PECVD SiO_2 | EBL patterning/wet etching of ~tens of nm holes | MOCVD growth of nanowire arrays

- Substrate patterning:
  - SiO_2 (30nm) deposition on InP (111)A substrate
  - Electron beam lithography and wet chemical etching to open holes on the SiO_2
- MOCVD growth
  - Growth temperature, gas flow rate and group V(PH_3) /group III (TMIn) ratio

MOVPE (MOCVD)

SAE growth of InGaAs/InP quantum wells based on WZ InP nanowires

High T_g (~700 °C) and low V/III ratio (~80)

Q. Gao et al., Nano Lett., 14, 5206 (2014).

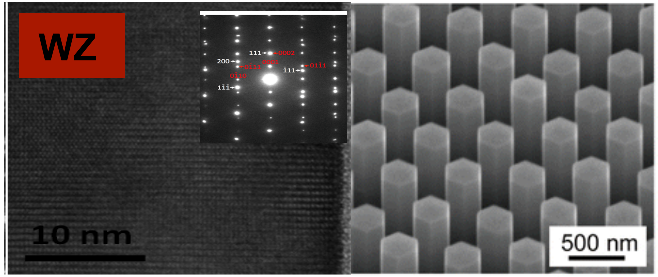

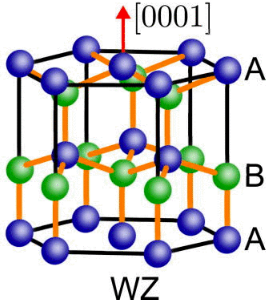

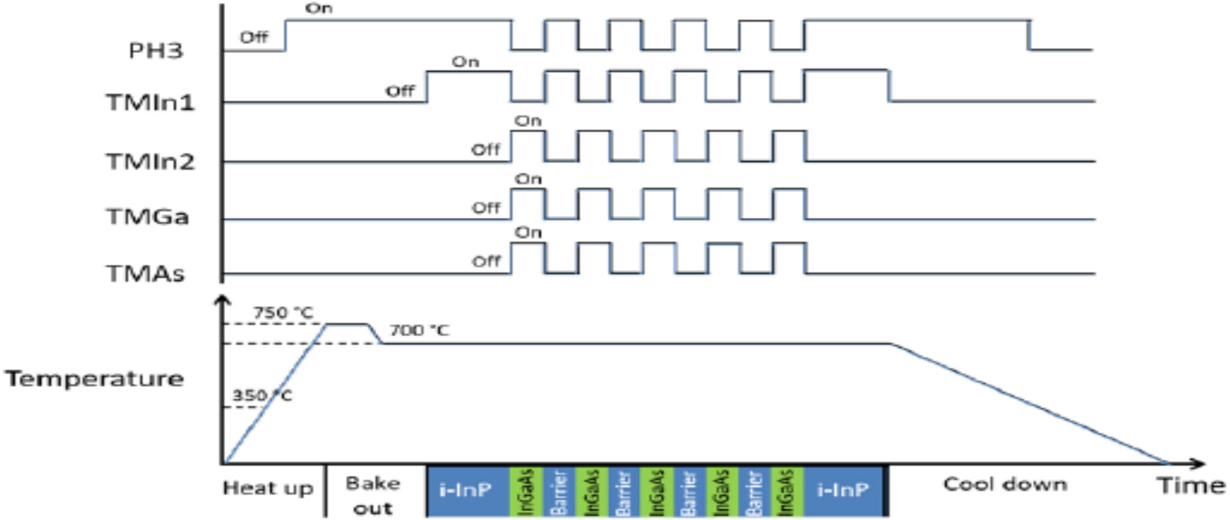

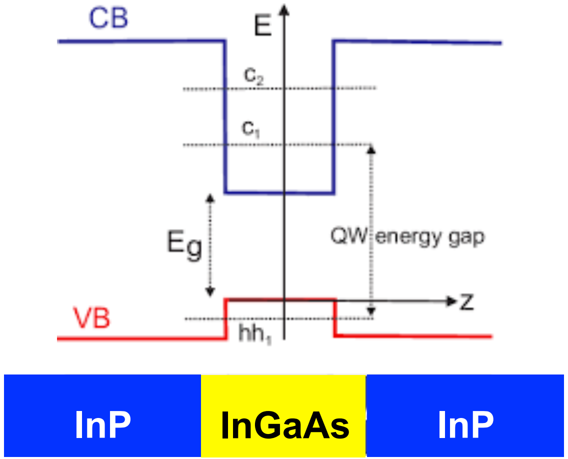

SEM of Single QW

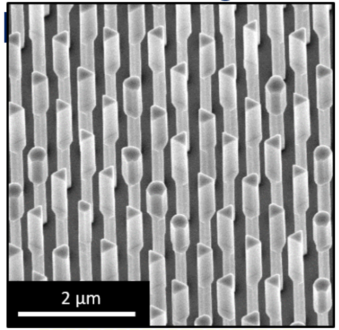

STEM image of NW

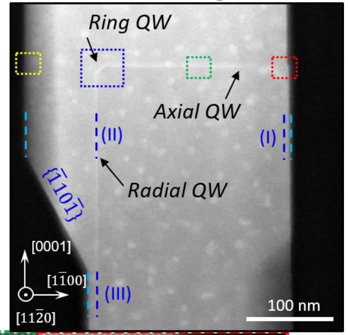

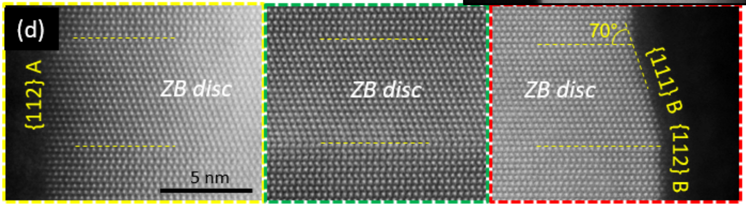

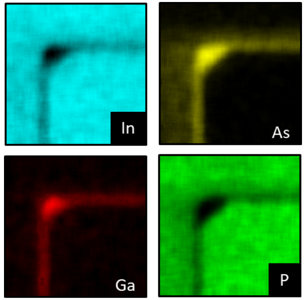

EDX mapping image from QW corner

- QW consists of three components: radial, ring and axial QWs.
- When InGaAs layer is grown on WZ InP nanowire, the radial InGaAs layer could adopt WZ structure from the core; axial InGaAs layer tends to form a more thermodynamically favorable ZB structure due to less surface energy consumption.
- This leads to different growth rate at different NW facets, creating the inclined facet as well as the facet evolution into diverse side facets and NW morphologies.

I. Yang *et* al., ACS Nano 12, 10374 (2018).

Optical property of InGaAs/InP QW nanowire

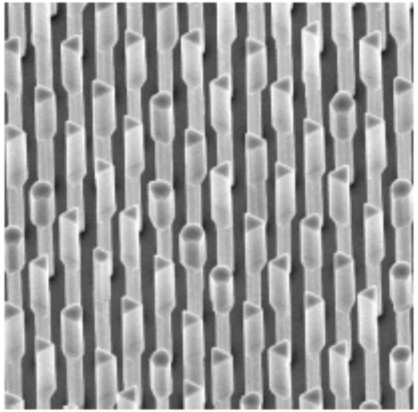

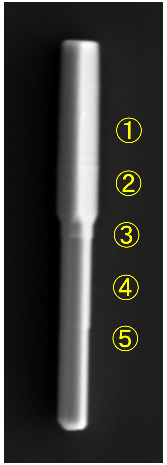

Shortest wavelength is originated from the radial QW while the longer wavelengths are from the ring or axial QW.

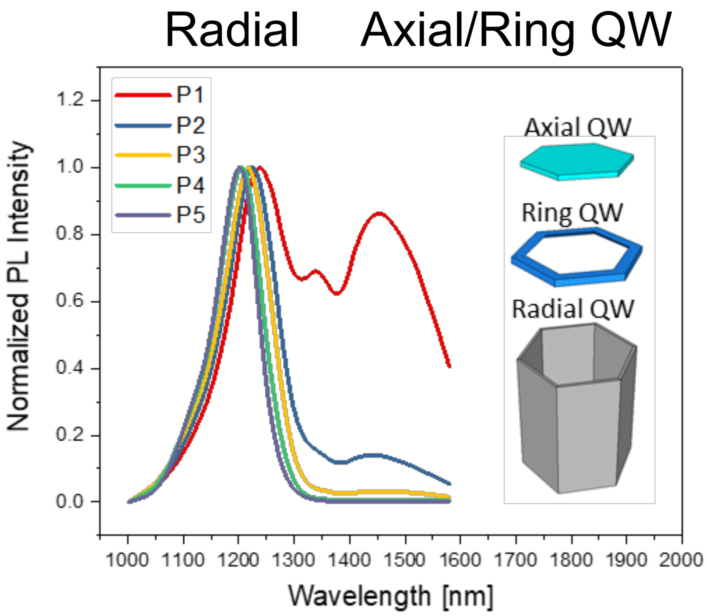

Position dependent Photoluminescence

FDTD Simulation of light extraction in single vertical NW

NW with inclined facet

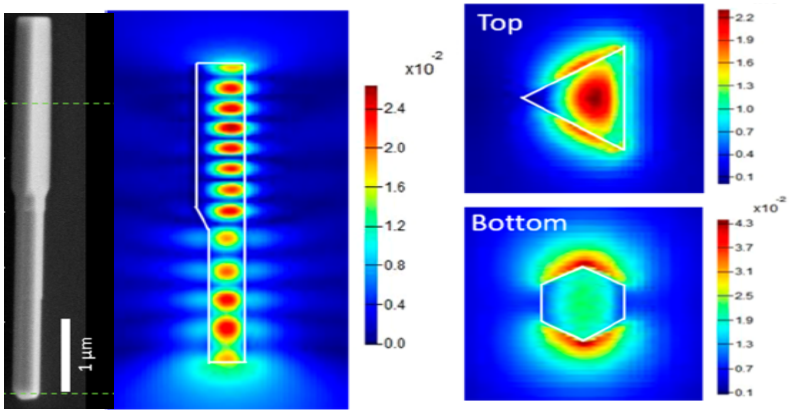

Light extractions to the top (triangle), bottom (hexagon), and the sides are 13.5, 37.9 and 45.2%, respectively.

NW with no inclined facet

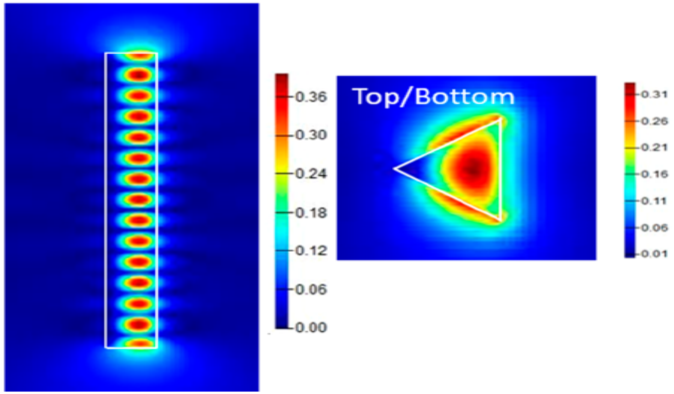

Light extractions to the top, bottom, and the sides are 25.3, 30.9, and 43.8%, respectively.

- The inclined lateral facets cause the disruption of optically resonant mode which leads to significant optical loss through the sidewall of NWs.
- Hexagonal facet has higher light extraction than triangular facet.

Y. Yang et al, Nano Energy 71, 104576 (2020).

Structural Transition in Indium Phosphide Nanowires

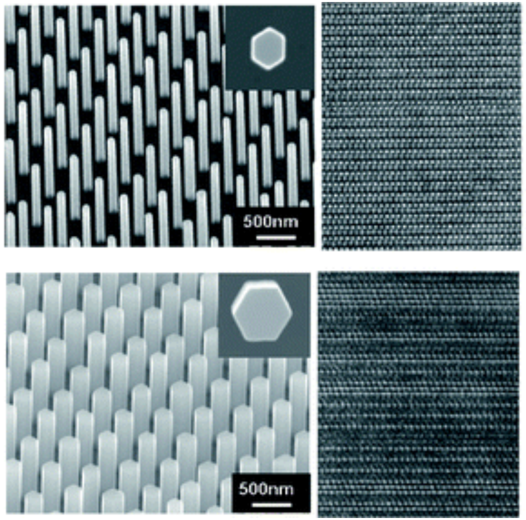

WZ facets: (higher T_g and lower V/III ratio)

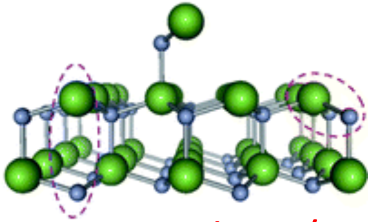

Mixed WZ/ZB facets: (lower T_g and higher V/III ratio)

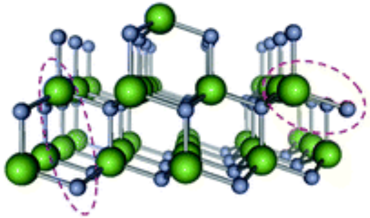

- The direction of the hexagon is different for the two types of nanowires, the facets are $\{1\bar{1}00\}$ of the surface of WZ and $\{1\bar{1}0\}$ of ZB in nanowires.
- Surface termination and sidewall surface energy play important role on the crystal structure transition of InP NWs.

Y. Kitauchi et al, Nano Lett. 10, 1699 (2010).

ZB InP Nanowire Growth (low growth T and high V/III)

V/III ratio Dependent Growth (T ~595 ℃)

V/III~297

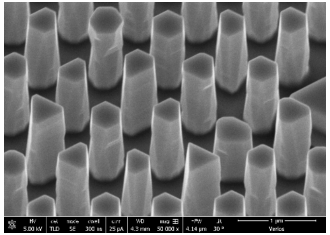

V/III~600

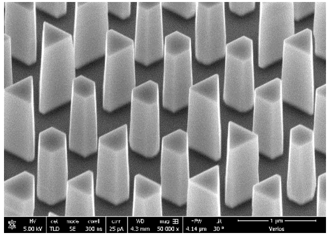

V/III~952

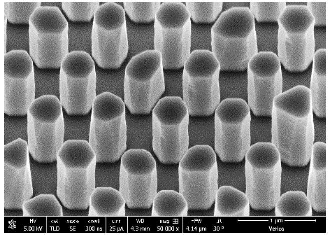

V/III~3186

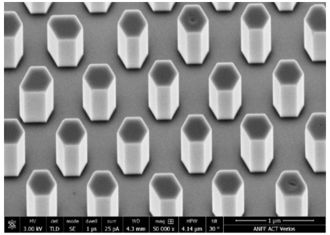

Temperature Dependent Growth (V/III ~3186)

T~580℃

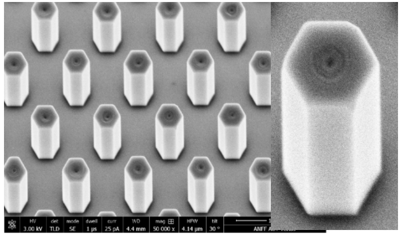

T~595℃

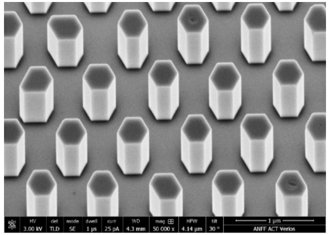

T~610℃

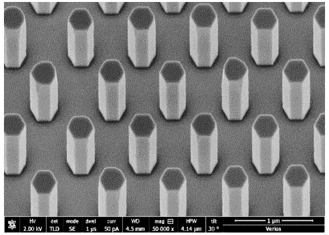

Optimized condition

T~625℃

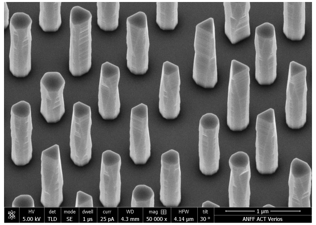

ZB InP Nanowire Characterisation

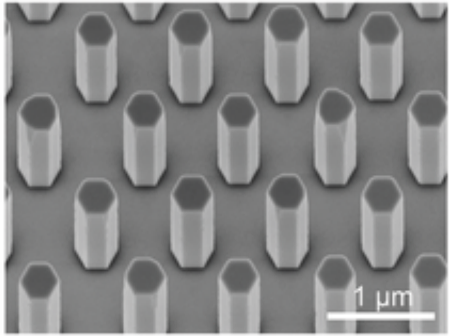

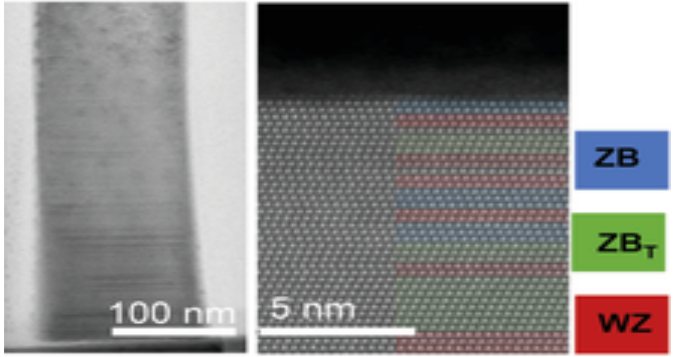

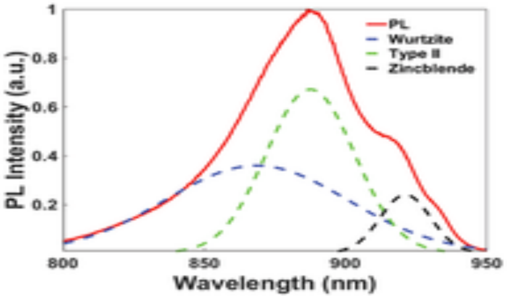

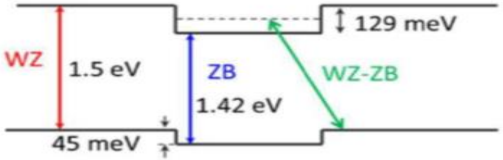

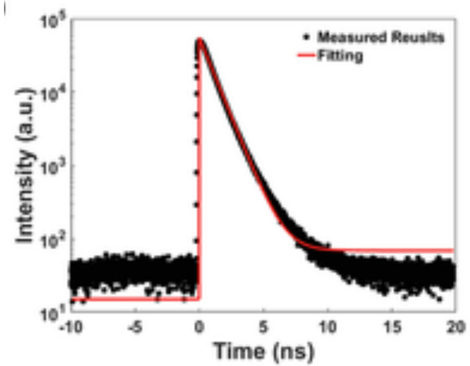

~ns minority carrier lifetime

- Mixed ZB/WZ (polytypic) structure
- High density of stacking faults
- Smooth {110} sidewalls
- ~ 1 ns lifetime

F. Zhang et al, Adv. Func. Mater. 202103057, 2021.

Australian National University

TMOS
ARC CENTRE OF EXCELLENCE FOR TRANSFORMATIVE META-OPTICAL SYSTEMS

High uniformity and high yield InGaAs/InP multi-QW Nanowires

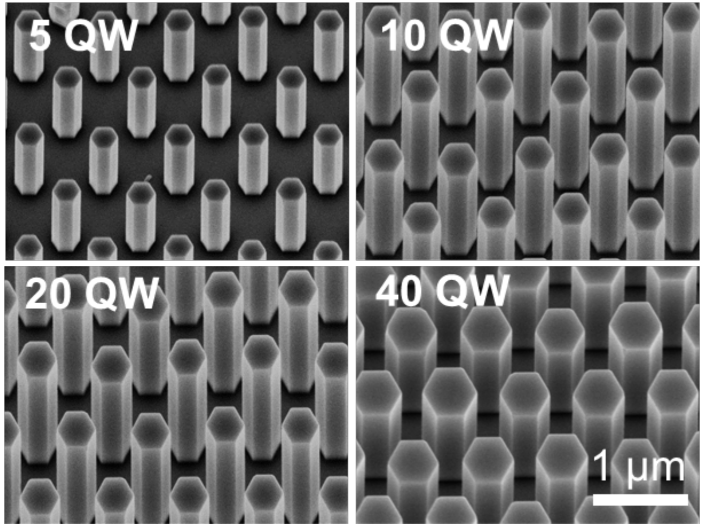

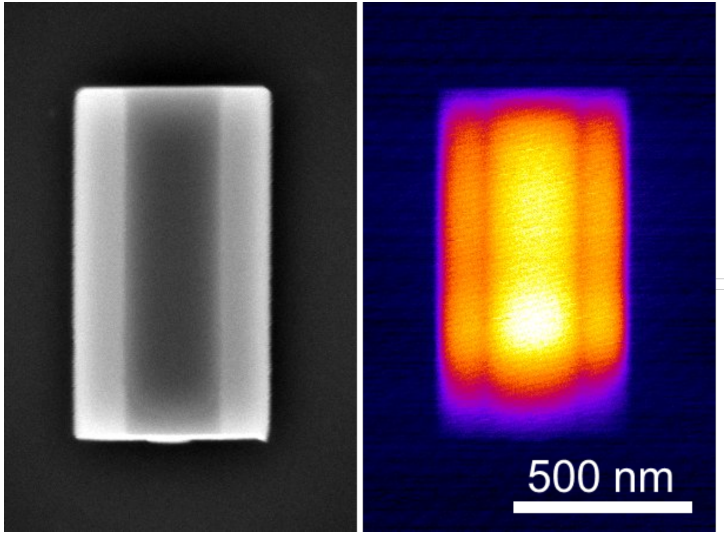

{110} faceted InP nanowire based QW growth

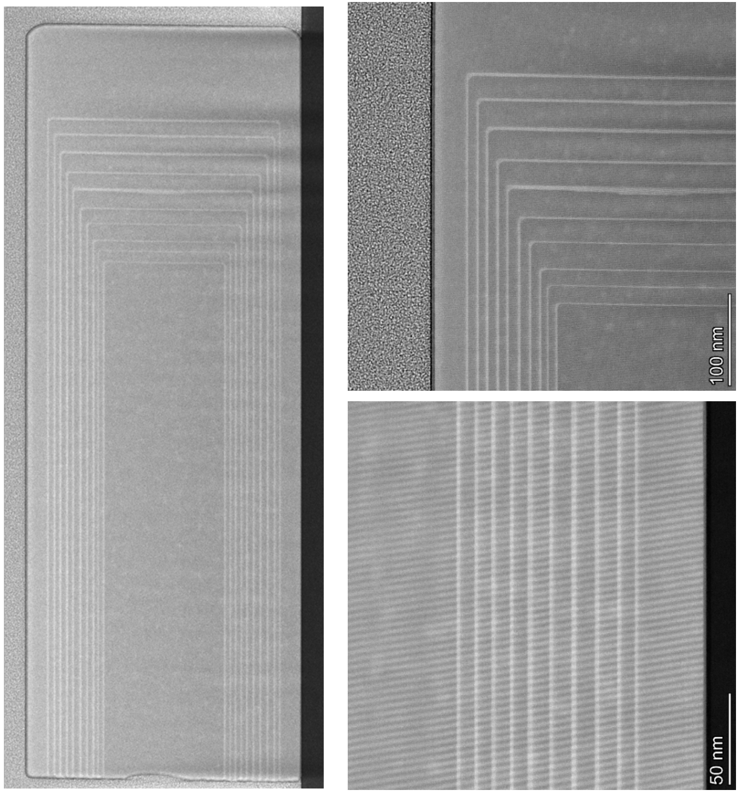

NW vertical cross-section

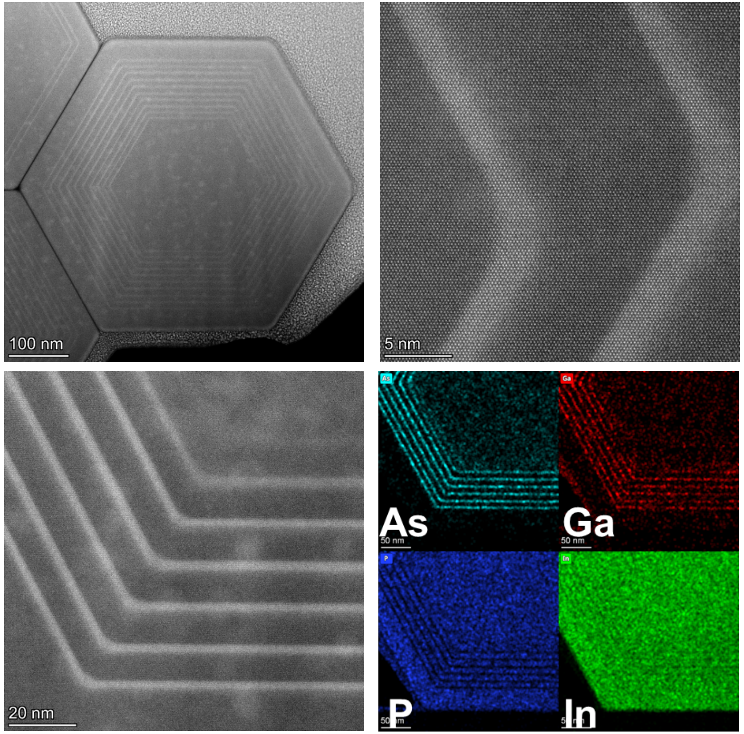

NW lateral cross-section

Optically pumped lasing from single QW-NW

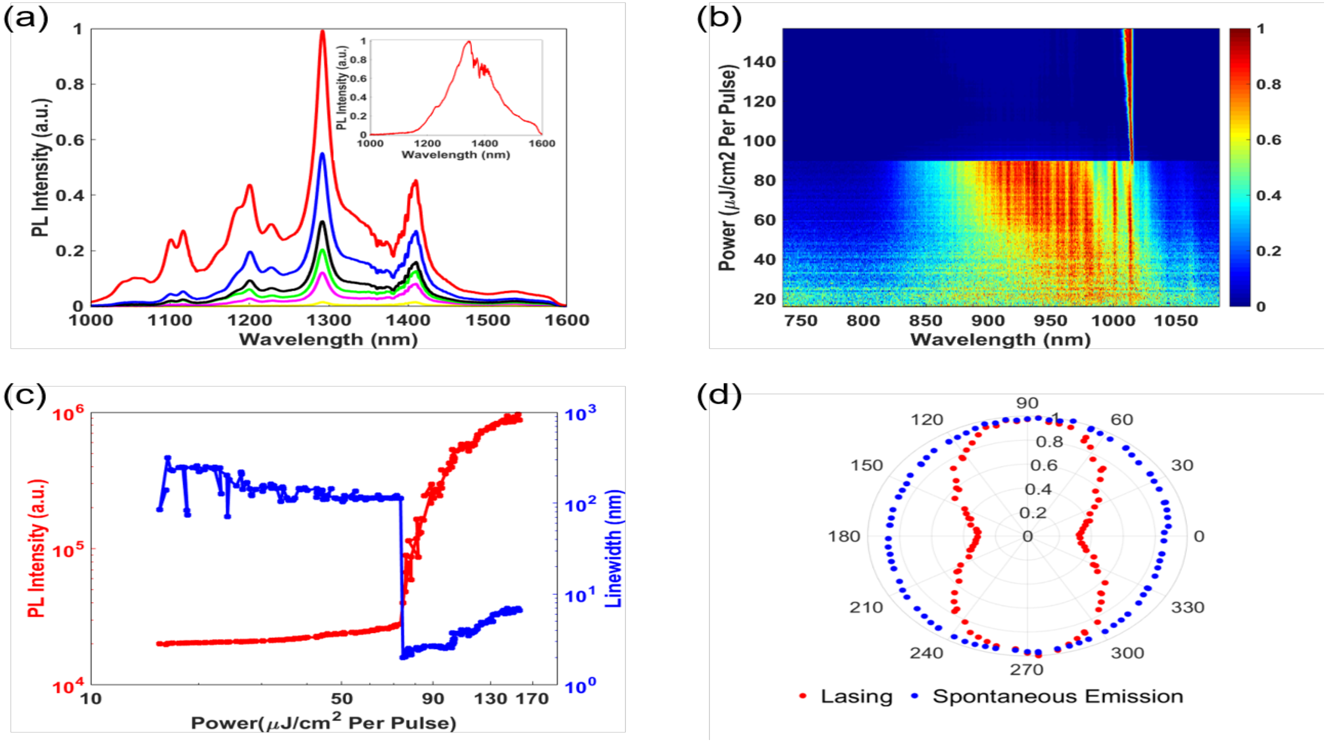

F. Zhang et al, Adv. Func. Mater. 202103057, (2021).

QW-NW Array LEDs

Australian National University

TMOS — ARC Centre of Excellence for Transformative Meta-Optical Systems

p-i-n InGaAs/InP 1-QW Nanowire

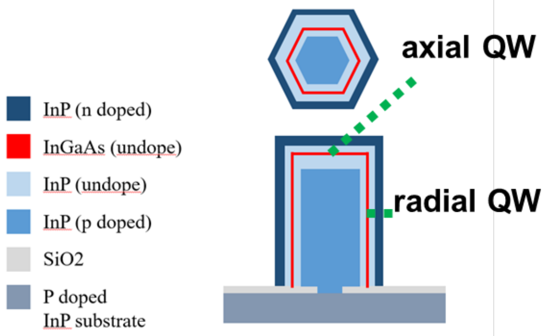

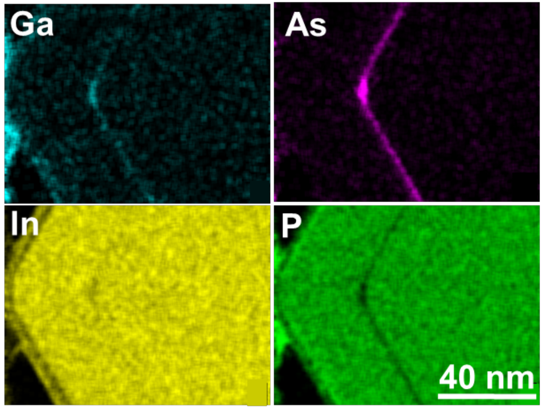

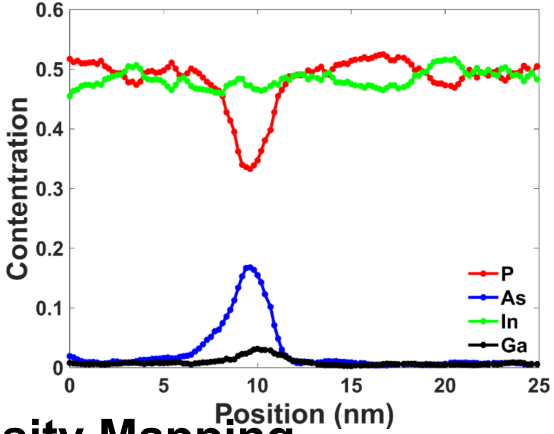

SEM

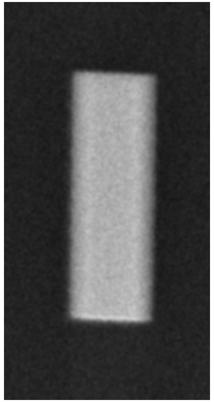

CL Spectra Mapping

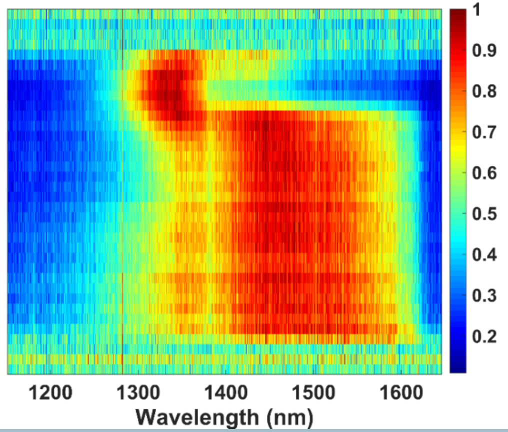

CL Intensity Mapping

1250 ~ 1350 nm 1450 ~ 1550 nm

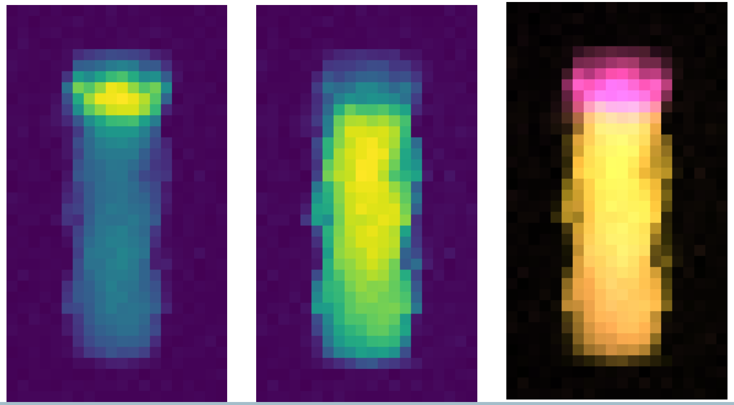

Australian National University

TMOS
ARC CENTRE OF EXCELLENCE FOR TRANSFORMATIVE META-OPTICAL SYSTEMS

Single QW-NW LED characterisation

Fabricated device

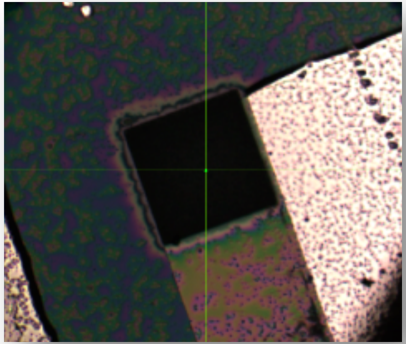

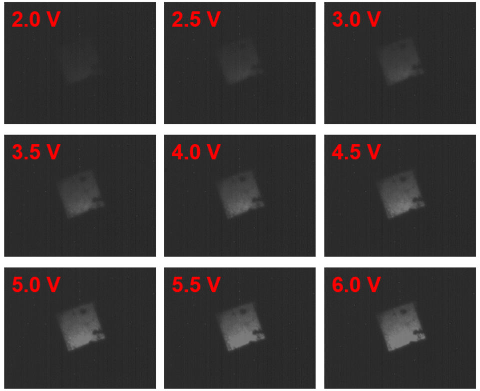

L-I-V curve

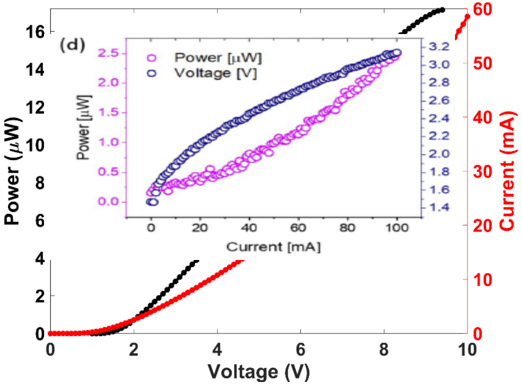

EL spectra

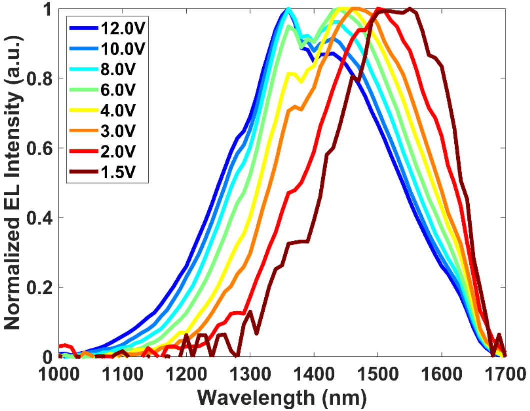

EL Modulation

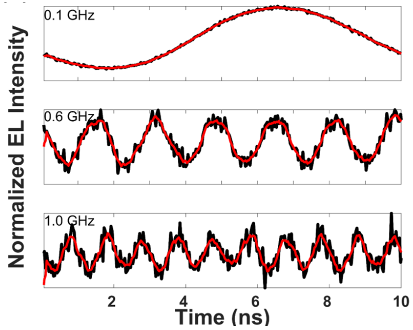

F. Zhang et al, Opto-Electronic Science 2, 230003 (2023).

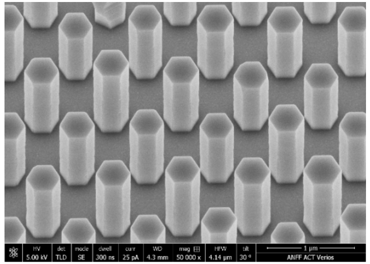

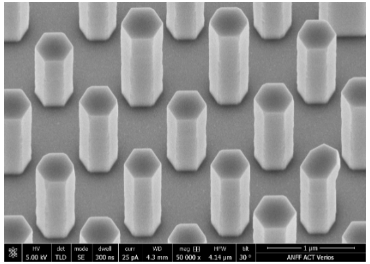

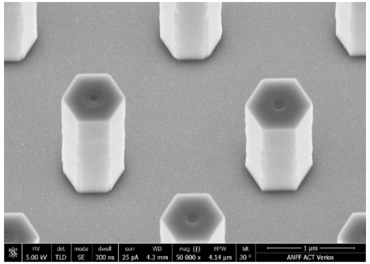

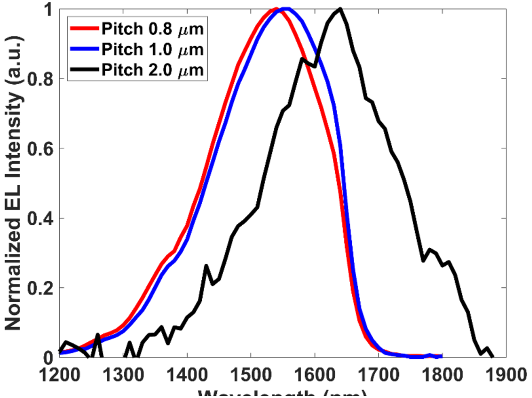

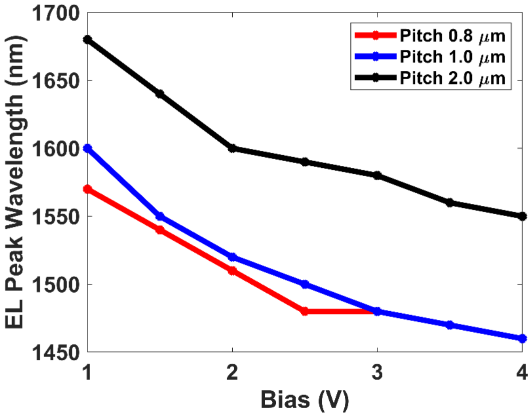

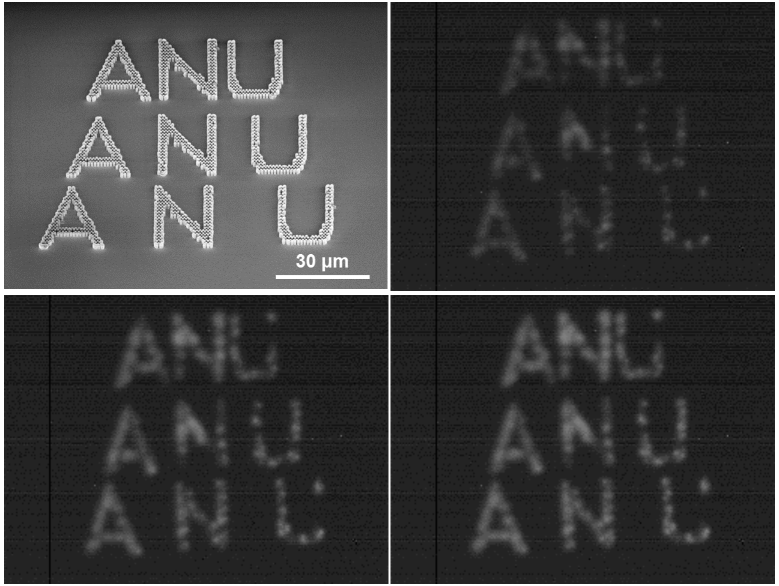

Promising for multi-wavelength, multi-pixel, individually addressable nanowire micro/nano LED arrays at low power consumptions.

F. Zhang et al, Opto-Electronic Science 2, 230003 (2023).

InGaAs/InP QW-NW NIR Photodetector

- Extended absorption to telecommunication wavelength
- Core-shell structure induces short carrier transportation distance leading to high gain and responsivity

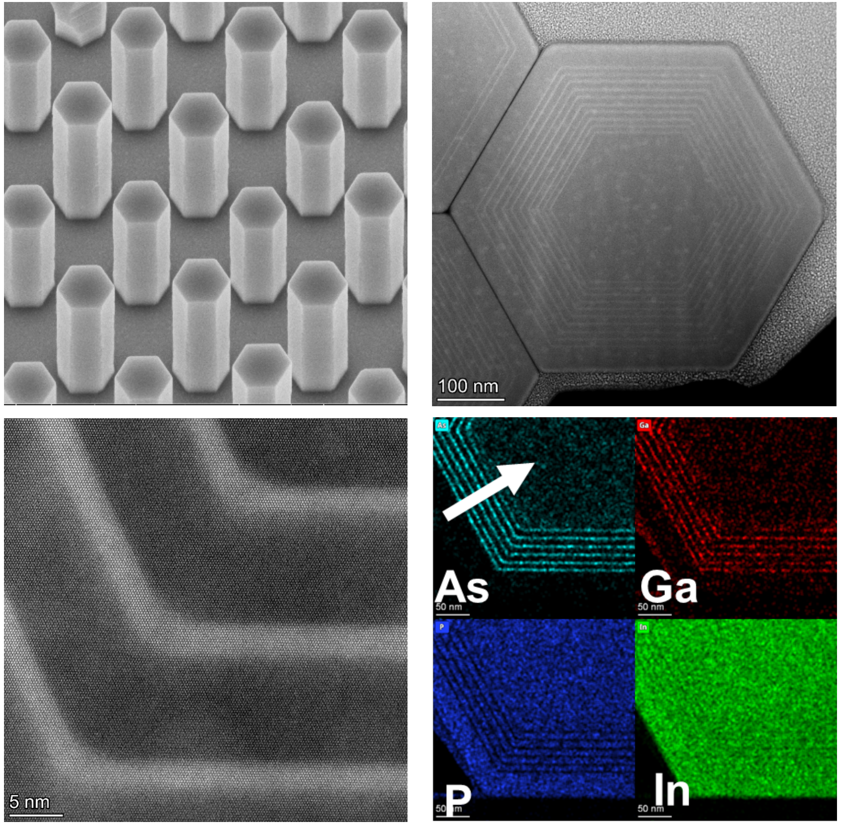

n-i-n InGaAs/InP MQW nanowire detector

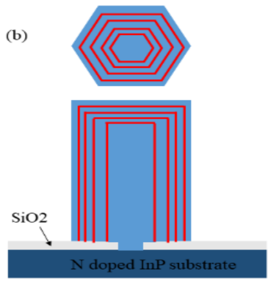

Photocurrent spectrum

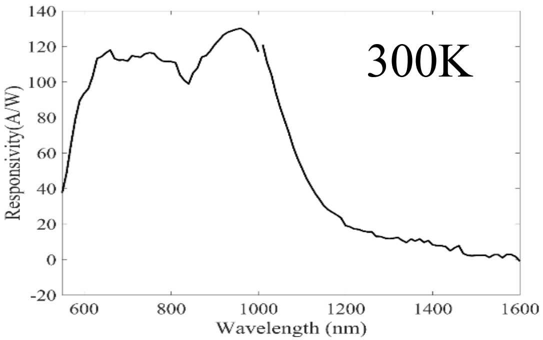

Power dependent responsivity

~2175 A/W @ 980nm,1.9 nW, 1.5 V

~14.5 A/W @1550 nm, 117 nW, 1.5V

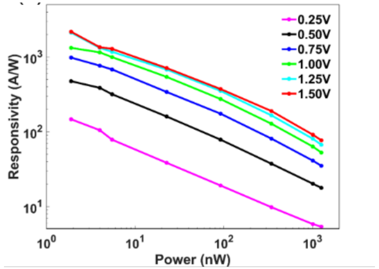

Photocurrent modulation

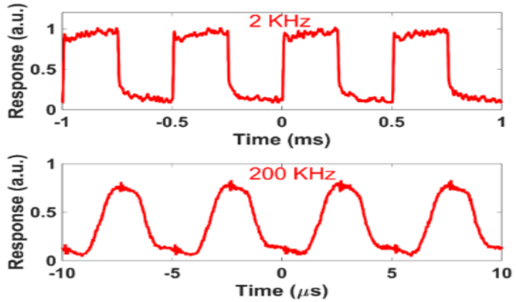

3dB frequency ~ 20KHz

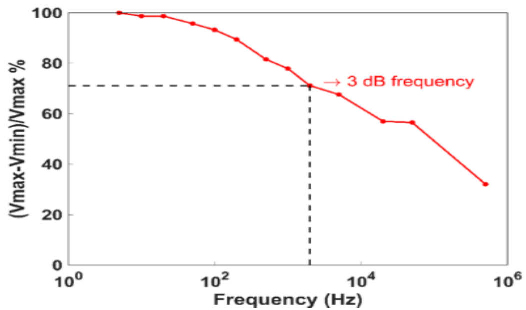

F. Zhang et al, Adv. Func. Mater. 202103057, (2021).

Australian National University

TMOS ARC CENTRE OF EXCELLENCE FOR TRANSFORMATIVE META-OPTICAL SYSTEMS

Nanowire Array Gas Sensors

Gas sensing

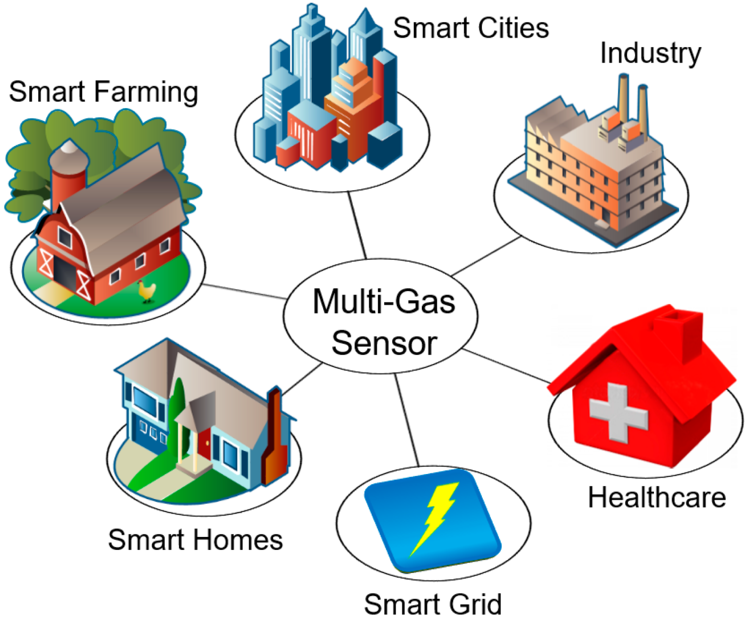

Current gas sensing methods

Gas chromatography - mass spectrometry

Ion mobility spectrometry

Limitations

- Require specialized equipment
- Time-consuming
- Difficult to realize the miniaturization

Nano material/structure based chemiresistive sensing

- Miniaturisation (or reducing the size of the sensors to the micro- or nano-scale) leads to:
  - a better signal-to-noise ratio as well as lower costs
  - large surface-to-volume ratio and thus increased active sensing area
  - increase of sensing speed
  - large-scale integration
  - Low power/self-powered operation

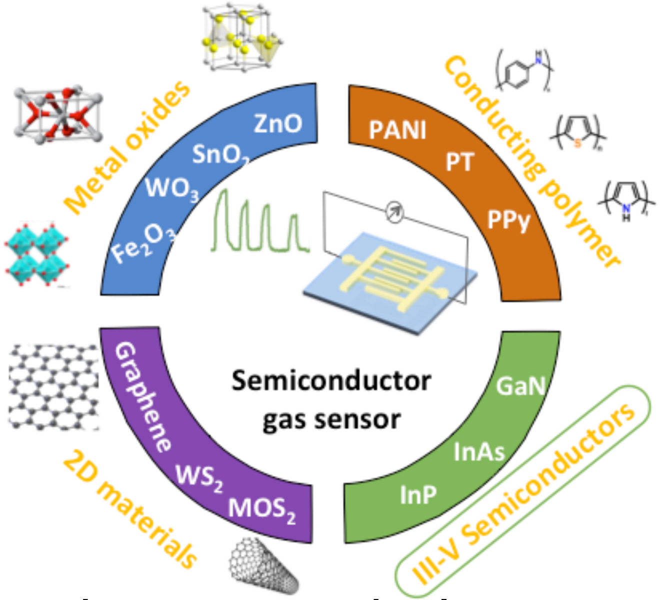

- Nanowire chemiresistive or FET biosensors have been extensively investigated for real-time, label-free detection of a variety of biomolecule disease markers, such as proteins, nucleic acid, and viruses.

InP single nanowire biosensors

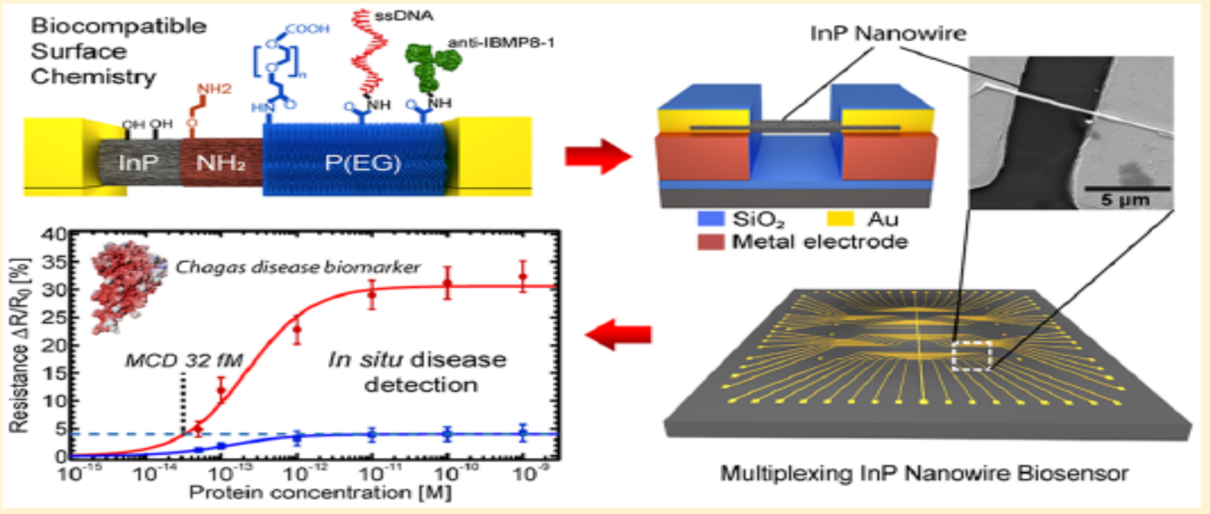

P. Arora et al, Appl Nanosci 3, 363 (2013).

Through tailored biofunctionalization, the single InP NW devices provide ultrahigh label-free detection sensitivities (~ 1fM) for specific DNA sequences, and for a Chagas Disease protein marker.

Challenges: accurate NW alignment, fabrication and reliability.

Nanowire array biosensors

- Nanowire chemiresistive sensors have been extensively investigated for real-time, label-free detection of a variety of biomolecule disease markers, such as proteins, nucleic acid, and viruses, as well as extracellular and intracellular sensing.

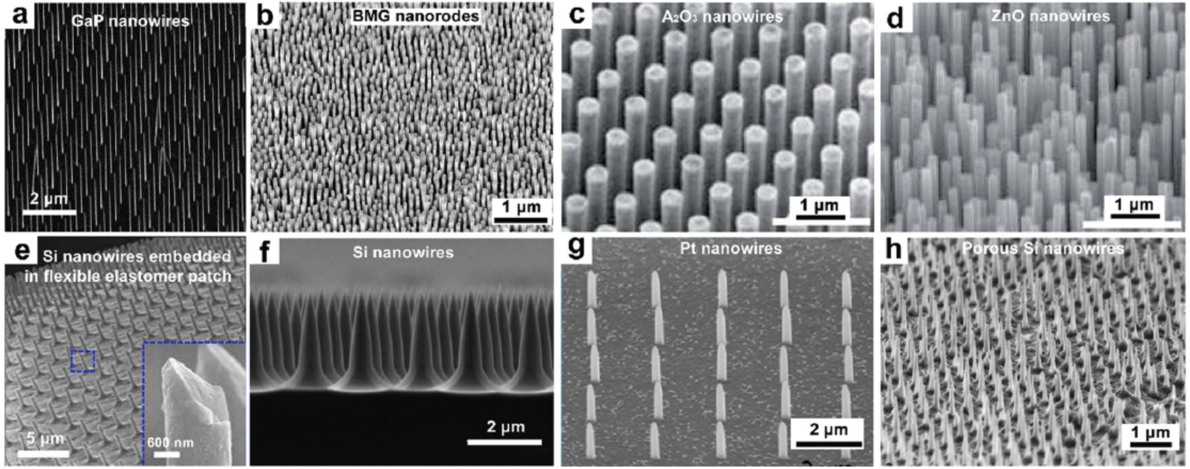

J. Mater. Chem. B, **8**, 7609 (2020).

Not much work on nanowire array (in particular III-V compound semiconductor based) gas sensors!

NO_2 gas sensors for environmental monitoring

- The latest research shows that vehicle emissions (a mix of pollutants including fine particulate matter (PM2.5) and nitrogen dioxide (NO_2)) in Australia may cause (https://www.unimelb.edu.au/newsroom/news/2023/february/vehicle-emissions-may-cause-over-11,000-deaths-a-year,-research-shows):
  - 11,105 premature deaths in adults per year, ten times more than road accidents
  - 12,210 cardiovascular hospitalisations per year;
  - 6,840 respiratory hospitalisations per year;
  - 66,000 active asthma cases per year

- During 2019 alone, almost two million cases worldwide of new childhood asthma were estimated to be due to nitrogen dioxide pollution - Children living in households that use gas stoves for cooking are 42% more likely to have asthma. (https://www.health.harvard.edu/blog/have-a-gas-stove-how-to-reduce-pollution-that-may-harm-health-202209072811)

III-V semiconductor NO_2 sensors

- NO_2 sensor based on InP epitaxial thin layers: 80 °C, non-reproducible up to 50ppm, slow response time

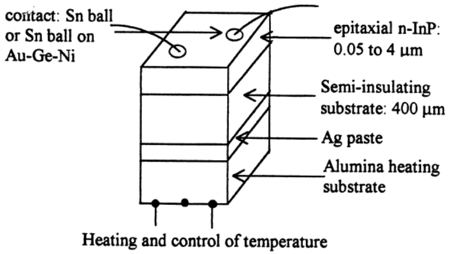

Fig. 1. Experimental gas sensor device.

80 °C

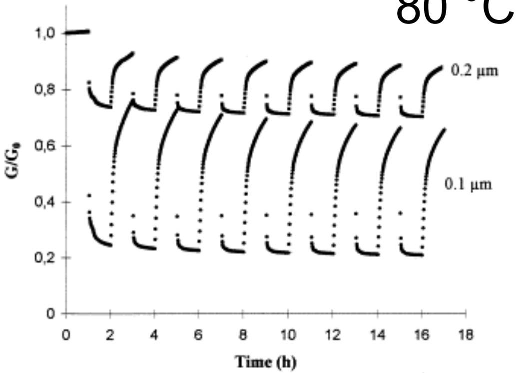

Thin Solid Films 348, 266 (1999).

- DFT calculations: 2D-InP_3 allotrope (δ-InP_3) shows strong chemical adsorption and charge transfer ability with NO_2.

W. C. Yi, et al, J. Mater. Chem. 7, 7352 (2019).

InAs nanowire array: non-stable response

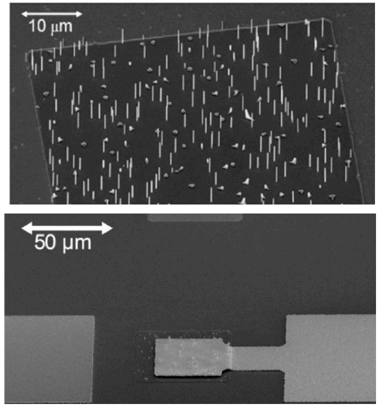

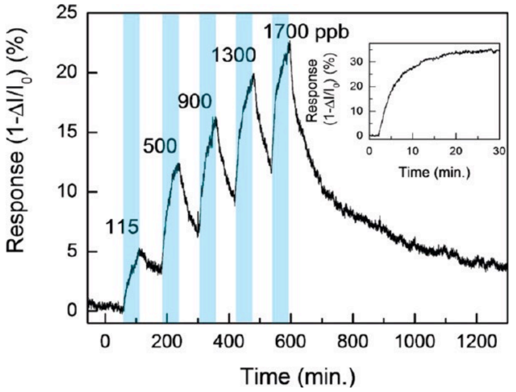

Nano Lett. 10, 2412 (2010).

III-V semiconductor NO_2 sensors

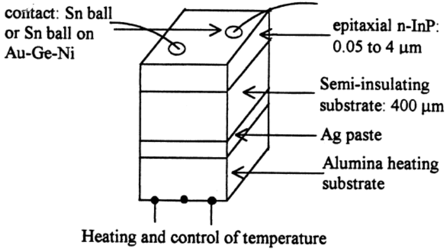

Fig. 1. Experimental gas sensor device.

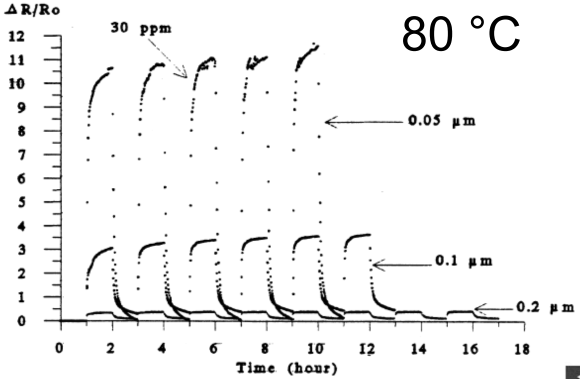

80 °C

InAs nanowire array

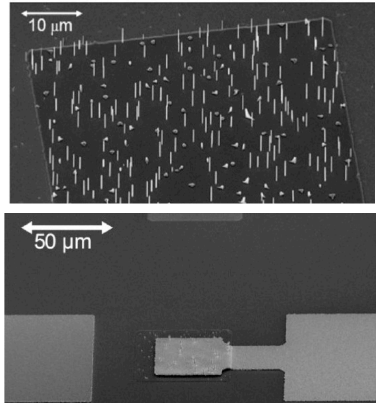

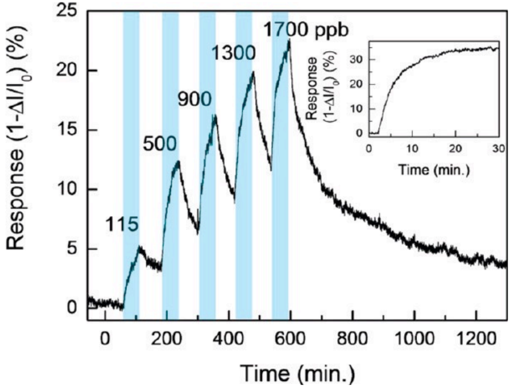

NO_2 sensor based on InP epitaxial thin layers

Thin Solid Films 348, 266 (1999).

DFT calculations: InP shows strong chemical adsorption and charge transfer ability with NO_2.

W. C. Yi, et al, J. Mater. Chem. 7, 7352 (2019).

NO_2 sensor based on InP NW arrays

Nano Lett. 10, 2412 (2010).

NO_2 emission & health

- The latest research shows that vehicle emissions (a mix of pollutants including fine particulate matter (PM2.5) and nitrogen dioxide (NO_2)) in Australia may cause (https://www.unimelb.edu.au/newsroom/news/2023/february/vehicle-emissions-may-cause-over-11,000-deaths-a-year,-research-shows):
  - 11,105 premature deaths in adults per year;
  - 12,210 cardiovascular hospitalisations per year;
  - 6,840 respiratory hospitalisations per year;
  - 66,000 active asthma cases per year
  - traffic pollution causes ten times more premature deaths than road accidents, which killed 1,123 people in 2021
- During 2019 alone, almost two million cases worldwide of new childhood asthma were estimated to be due to nitrogen dioxide pollution - Children living in households that use gas stoves for cooking are 42% more likely to have asthma. (https://www.health.harvard.edu/blog/have-a-gas-stove-how-to-reduce-pollution-that-may-harm-health-202209072811)

InP NW array fabrication: top-down etching

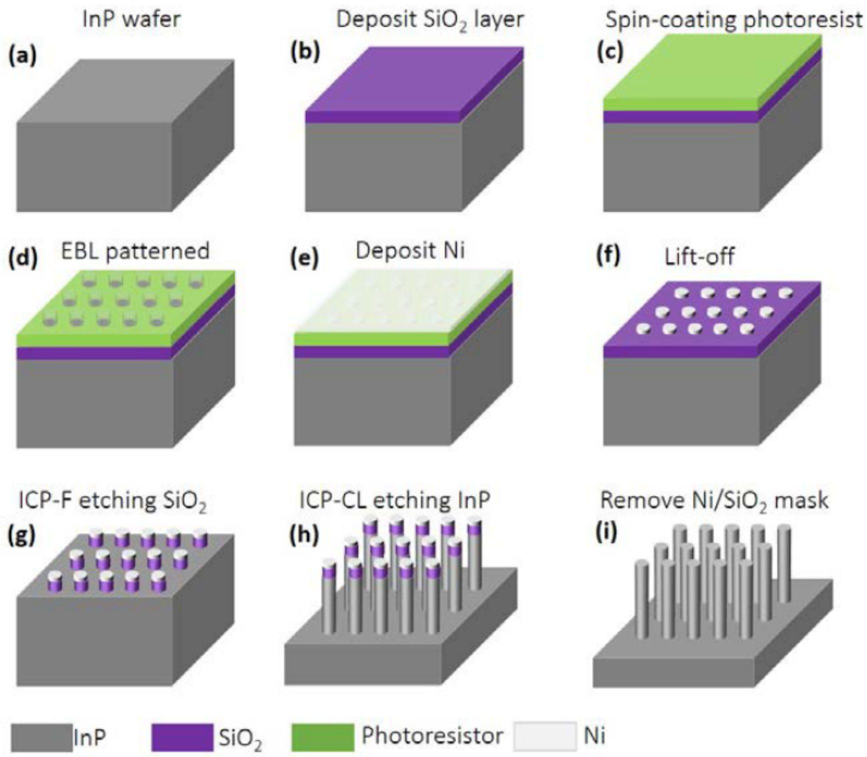

InP NW array fabrication

Diameter 100 nm | Diameter 200 nm | Diameter 300 nm

Interspace 1000 nm

Diameter 100 nm

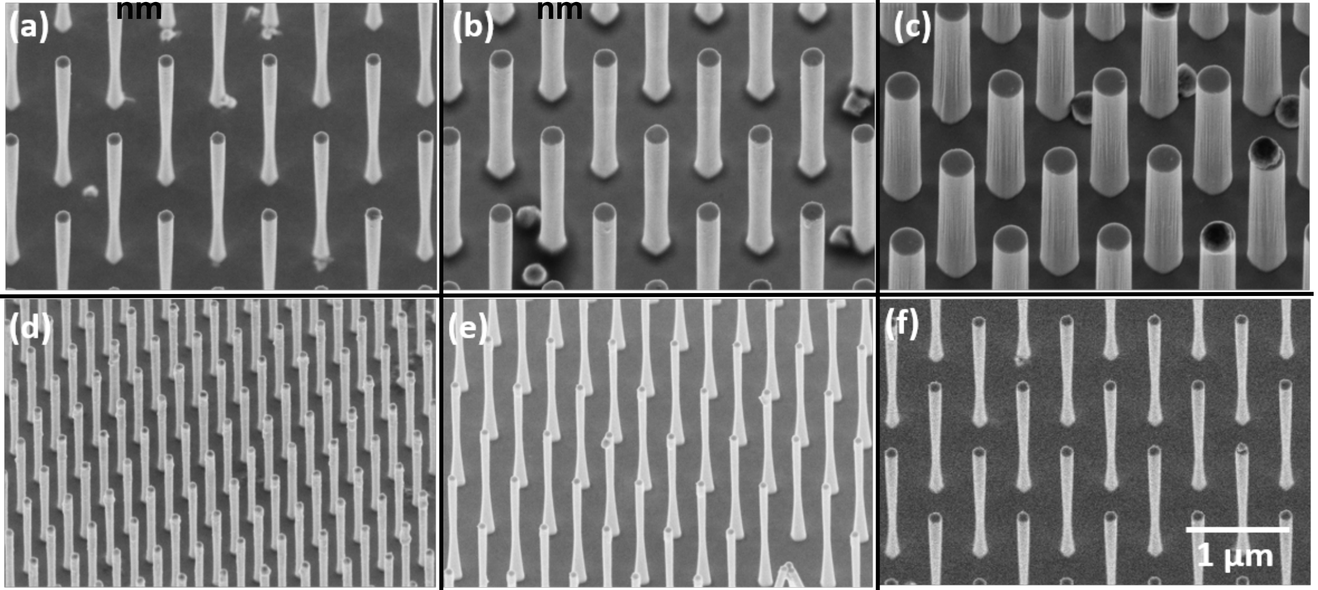

Interspace 400 nm | Interspace 600 nm | Interspace 800 nm

InP NW array NO_2 sensor fabrication

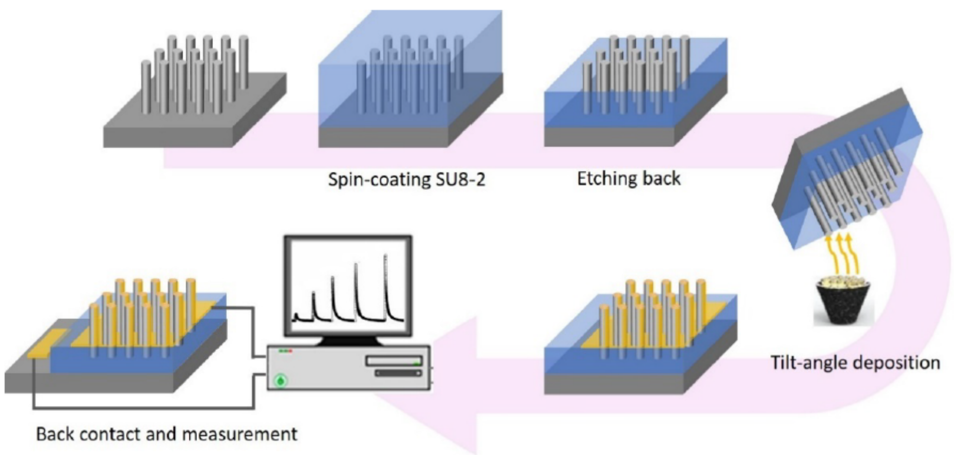

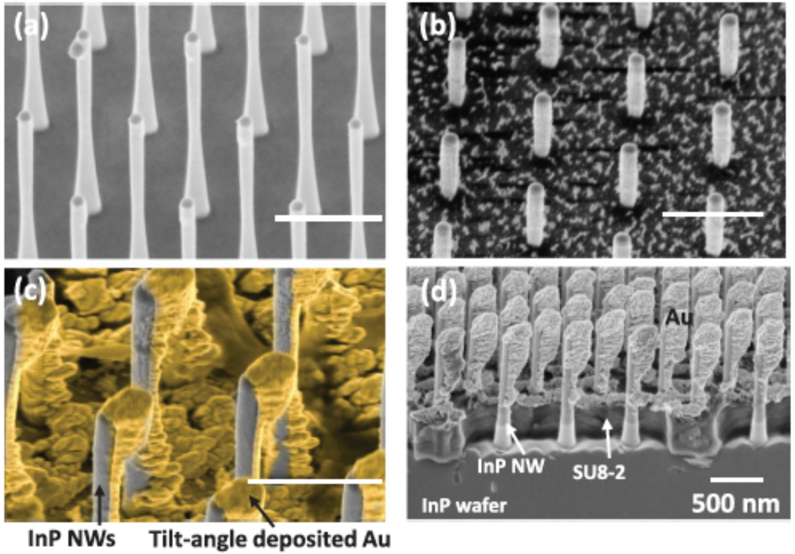

NW geometry related sensing performance

Spacing variation

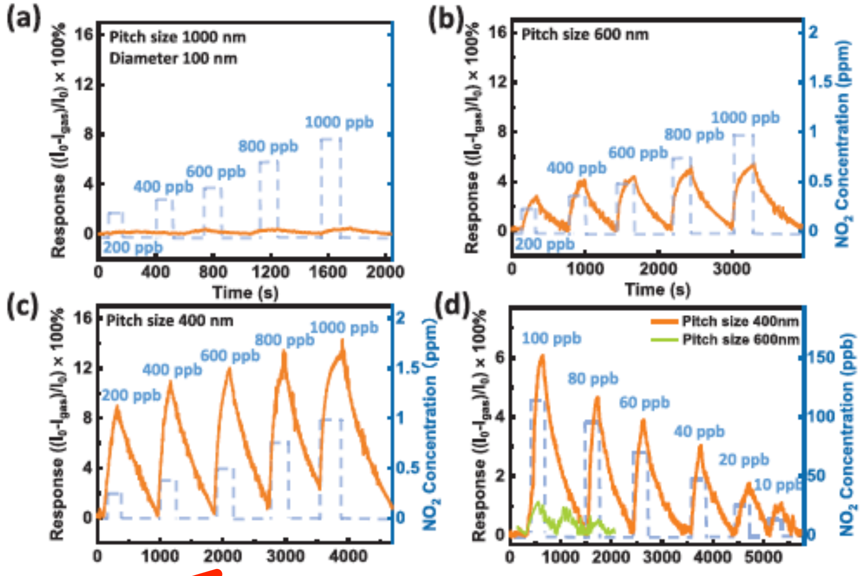

$$NO_{2(gas)} \leftrightarrow NO_{2(ad)}$$

$$NO_{2(ad)} + e^- \leftrightarrow NO^-_{2(ad)}$$

Diameter variation

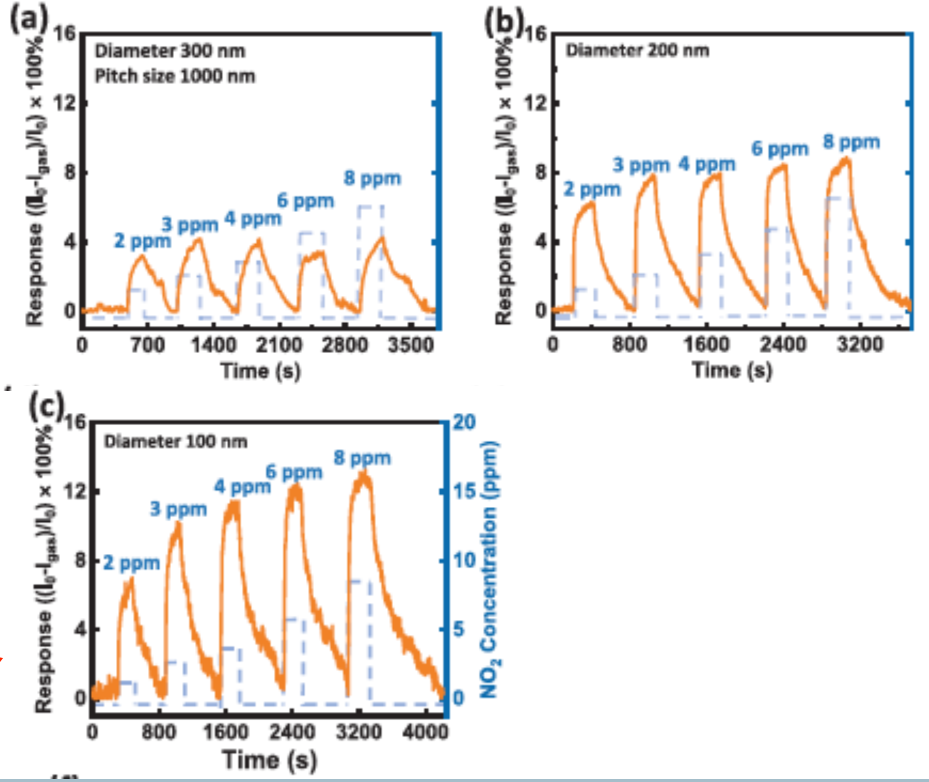

Limit of detection (LOD), selectivity and air stability

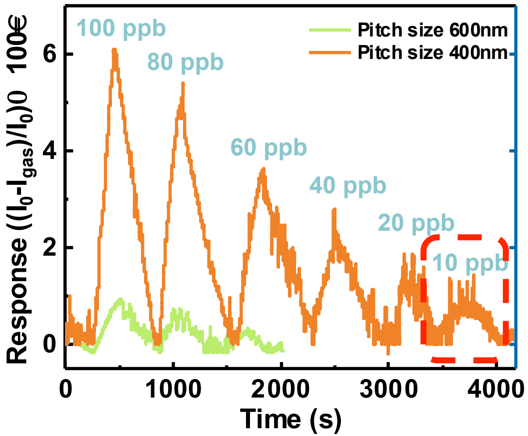

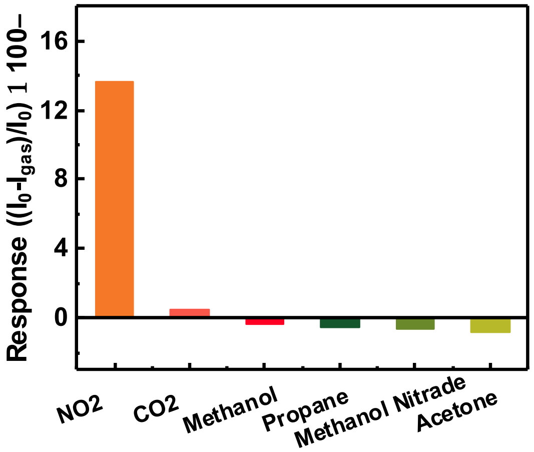

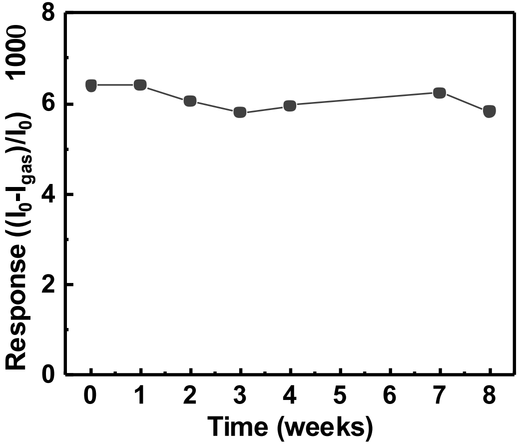

Performance comparison

Material/structure	Sensitivity [%] (1 ppm)	LOD [ppm]	Response/recovery time	Working temperature [°C]
InP-NWs	12.9	0.01	43/127 s	25
n-InP-epitaxy layer	6	0.1	1800/3600 s	80
InAs/InP-NWs	21	0.03	–	50
InAs-NWs	17	0.15	2400/2200 s	25
Pd-In_2O_3-NWs	6	1	71/100 s	110
ZnO	12	0.03	–	150
ZnO/Graphene	21	0.05	182/234 s	110
SnO_2-NWs	81	0.05	–	300
Pt/WO_3	18	0.5	198/225 s	400
MoS_2/Graphene	12	0.05	–	200
Ni-MOF	85	0.5	2700/-s	50

By investigating the NW geometry related gas adsorption and electron transfer/depletion process, high performance NO_2 sensing with ppb level of limit of detection at room temperature, and high selectivity and stability have been achieved.

S. Y. Wei et al, Adv. Func. Mater. 32, 2107596 (2021).

Self-powered nanowire array NO_2 sensor

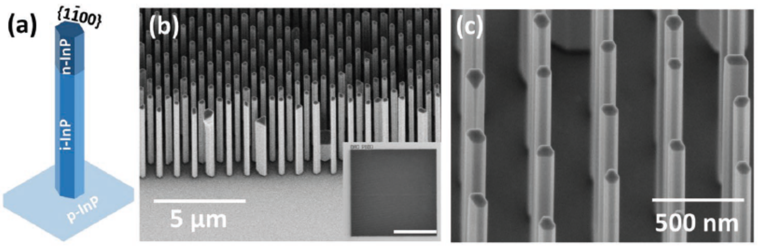

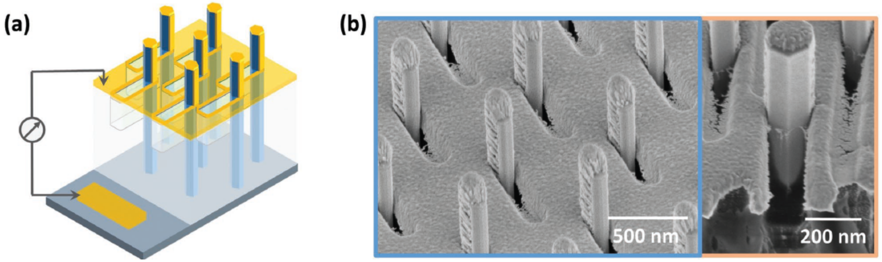

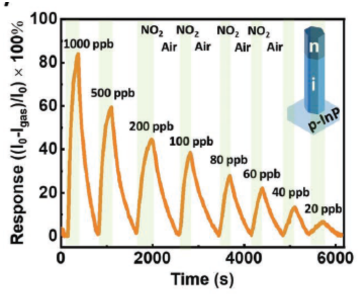

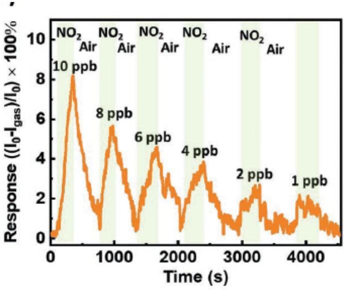

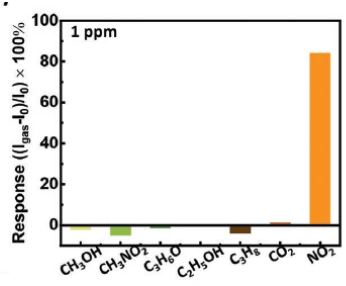

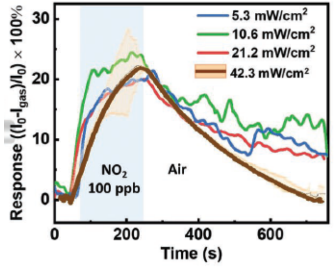

S. Y Wei etc, Advanced Materials, https://doi.org/10.1002/adma.202207199 (2022).

On-field sensing measurement based on the self-powered NO_2 sensor

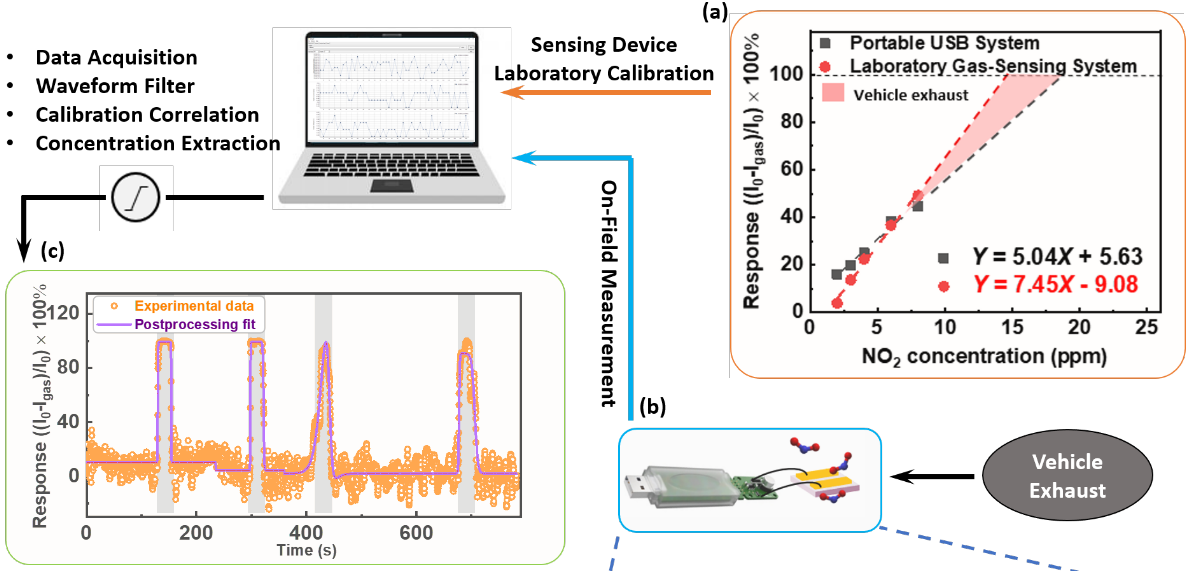

(d)

Time Start (s)	Time End (s)	Calculated Concentration (ppm)
130	154	16.5 ± 2.0
298	322	16.6 ± 2.0
429	442	16.5 ± 2.0
677	706	15.2 ± 1.7

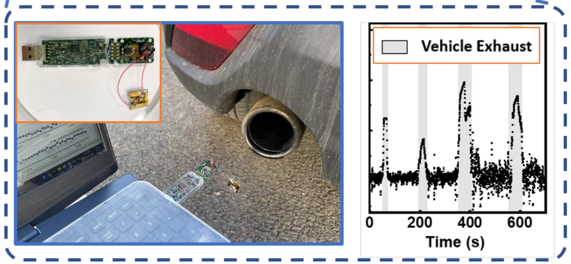

S. Y Wei et al, Advanced Materials, https://doi.org/10.1002/adma.202207199 (2022).

Australian National University

Acknowledgements

TMOS
ARC CENTRE OF EXCELLENCE FOR TRANSFORMATIVE META-OPTICAL SYSTEMS

- **Students/colleagues**

  F. L. Zhang, Yue Bian,S. Y. Wei, A. Bhat, Z. Y. Li, Y. Zhu, Z. Li, V. Raj, B. Karawdeniya, I. Yang, K. Peng, Q. Gao, X. M. Yuan, F. Wang, Y. Guo, S. Mokkapati, P. Caroff, J. Wong-Leung, H. H. Tan, and C. Jagadish

- **Australian National Fabrication Facility – ACT Node**

  L. Li, K. Vora, M. Lysevych, O. L. C. Lem, G. Vaidya, M. Lockery

- **Electronic Unit – Research School of Physics, ANU**

  D. Gibson, S. Marshall, M. Blacksel

- **Collaborators**

  A. Tricoli, K. Murugappan – ANU
  S. Kim, I. Aharonovich, M. Toth, F. Wang – University of Technology Sydney
  J. T. Qu, J. Cairney – University of Sydney
  W. W. Pan, L. Wen, L. Faraone – University of Western Australia
  M. Johnston, Hannah Joyce – Oxford Univ.
  P. Parkinson – Univ. Manchester
  Monica Allen, Jeffery Allen - Air Force Research Laboratory, Eglin AFB, Florida
  Weida Hu, Wei Lu – Shanghai Institute of Technical Physics

ANFF

AFOSR-AOARD

Australian Government
Australian Research Council

Australian National University

Conclusions

- III-V semiconductor nanowires offer great potentials for a range of device applications
- Highly uniform III-V quantum well nanowires have been achieved and optimised, promising for optoelectronic device applications in highly integrated PICs
- III-V nanowires are promising sensor platform for IoTs
- In-depth understanding and optimisation of III-V nanowire growth, structural, optical and electrical properties are essential for high performance nanowire based devices and systems

Thank you!